Synthetic Analogues of Cysteinate-Ligated Non-Heme Iron and Non-Corrinoid Cobalt Enzymes

Julie A. Kovacs*

Department of Chemistry, University of Washington, Box 351700, Seattle, Washington 98195

Received June 24, 2003

Contents

Julie Kovacs was born in East Lansing, Michigan (in 1959), received her undergraduate degree from Michigan State University (in 1981) and her Ph.D. from Harvard (in 1986), and did postdoctoral work at U.C. Berkeley. She has been on the faculty at the University of Washington in Seattle since 1988. She developed a passion for science as a result of lively discussions with her father, a theoretical physicist. Her interest in metalloenzymes developed while pursuing a Ph.D. with Richard Holm. Her research focuses on understanding the role played by sulfur in determining function in cysteinate-ligated non-heme iron enzymes. She approaches this problem via the synthesis of small molecular enzyme active site analogues which reproduce key spectroscopic features. Systematic alteration of the active site structure allows one to correlate structure with properties and function. In addition to her work, a love of the outdoors (both salt and mountain air), her husband (Steve), and her two children (Anna and Eric), inspires her to treasure each and every day.

1. Introduction to Non-Heme Iron Enzymes

Non-heme iron enzymes promote a number of important biological reactions, including serotonin,[1] leukotreine,[2] and DNA[3] synthesis. Most mononuclear non-heme iron enzymes contain iron ligated by oxygen and/or nitrogen ligands (Figure 1A).[4−6] Many of these enzymes promote dioxygen activation, resulting in the formation of highly reactive iron−peroxo ($Fe^{III}-OOH$, $Fe^{III}-O_2^-$)[7,8] or iron−oxo ($Fe^{IV}=O$ or $Fe^{V}=O$)[9] oxidation catalysts.[8] The flexible coordination environment of enzymes containing 2-His-1-carboxylate (N_2O)-ligated iron leaves room for substrate as well as dioxygen activation to occur at the metal site. In many cases, dioxygen binding does not occur until substrate has entered the active site cavity.[4−6,10] In the enzyme lipoxygenase, the active catalyst is an $Fe^{III}-OH$ that is capable of cleaving weak C−H bonds.[11−13] The property most important in promoting this H-atom abstraction chemistry is the redox potential, which favors the Fe^{II} oxidation state.[14−16] Relatively recently, a *new class* of *cysteinate sulfur-ligated* non-heme iron enzymes emerged. This new class includes nitrile hydratases (NHases),[17−28] superoxide reductases (SORs),[29−42] and peptide deformylases (PDFs).[43−45] The active site structures of these enzymes are compared with that of N_2O-ligated non-heme iron enzymes in Figure 1. Crystal structures are available for all three cysteinate-ligated non-heme iron enzymes—nitrile hydratase

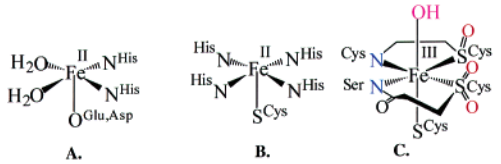

Figure 1. Active sites of 2-His-1-carboxylate (N_2O)-ligated non-heme iron enzymes (A) vs cysteinate-ligated nitrile hydratase (NHase; C) and superoxide reductase (SOR; B).

10.1021/cr020619e CCC: $48.50 © xxxx American Chemical Society
Published on Web 00/00/0000 PAGE EST: 23.8

BATCH: cr80a25 USER: slr69 DIV: @xyv04/data1/CLS_pj/GRP_cr/JOB_i80/DIV_cr020619e DATE: January 2, 2004

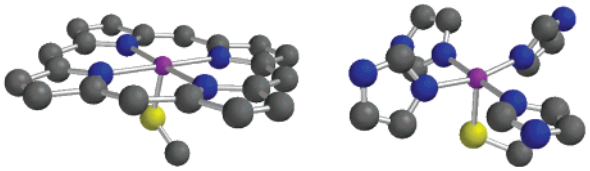

Figure 2. Comparison of the active sites of superoxide reductase (SOR) vs cytochrome P450.

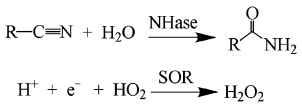

Figure 3. Reactions catalyzed by the metalloenzymes nitrile hydratase (NHase) and superoxide reductase (SOR).

(NHase),[25,26] superoxide reductase (SOR, vide infra),[34] and peptide deformylase (PDF).[46] Peptide deformylases contain a tetrahedral Fe^{II} ion ligated by one cysteinate sulfur, two histidine nitrogens, and a water.[46] As shown in Figure 1, SOR shares the N_2X triad (X = O, S) seen with the majority of non-heme iron enzymes, with a cysteinate (X = S; Figure 1B) replacing the more common carboxylate (X = O; Figure 1A) residue, and two histidines replacing two of the waters. Nitrile hydratase (Figure 1C) and SOR (Figure 1B) have in common an active site containing a cysteinate sulfur trans to the "substrate binding site". Two additional cysteinates ligate the iron of NHase (Figure 1C), completing one of the faces of an octahedron, with the remaining coordination sites occupied by two peptide amide nitrogens and either a hydroxide (pH = 9 form),[22,23,25,47] or NO (inactivated form).[24,26,48] Metal ion ligation by peptide amides is rare in biology. There are only two other examples of this ligation mode: the P-cluster of nitrogenase[49] and the bimetallic reaction center (the "A cluster") in acetyl CoA synthase (ACS).[50] As shown in Figure 2, the active site structure of SOR (in its reduced state) resembles that of the heme iron site of cytochrome P450. Both contain a cysteinate ligand trans to an open coordination site, with the four equatorial histidines of SOR resembling a broken-up porphyrin ring.[51]

An obvious question about the structure of this newer class of enzymes concerns the role that peptide amides and cysteinate sulfur ligand(s) might play in promoting function. The function of this new class of non-heme iron enzymes varies enormously from nitrile hydratation (Figure 3) by nitrile hydratases (NHases),[22,23,25−28,52] to the hydrolytic removal of a formyl "tag" by peptide deformylase (PDF),[44−46] to superoxide reduction (Figure 3) by superoxide reductases (SORs).[33,34,42,53] Peptide amides have been shown to stabilize metal ions in higher oxidation states[54−57] and favor structures with lower coordination numbers.[56,58] This may help to maintain an "open" exchangeable site at the NHase iron for substrate or hydroxide binding to occur. Cysteinate sulfur ligands are known to form highly covalent bonds to transition metals[59,60] and facilitate electron-transfer reactions.[61,62] As shown in this review, cysteinate sulfur ligands also help to stabilize Fe^{III} and make low-spin iron accessible in a non-heme environment.[63−65] The trans-coordinated cysteinate sulfur of the heme iron enzyme cytochrome P450 is thought to promote O−O bond cleavage, resulting in the formation of a reactive oxidation catalyst.[51,66−68] As described in this review, the trans-coordinated cysteinate sulfur of NHase has also been shown to play an important role in promoting reactivity, by promoting ligand dissociation at the trans site. Cysteinate sulfurs could also potentially provide an alternate site for reactivity to occur with dioxygen, peroxides, or even hydroxides (vide infra).[69−71] This review will primarily focus on synthetic functional and structural models for the cysteinate-ligated non-heme iron enzymes NHase and SOR. For additional review articles focusing on the more biological aspects of these enzymes, see refs 27, 28, 35, 72−77. For reviews focusing on NHase modeling studies, see refs 78 and 79. For reviews on nitrogen/oxygen-ligated non-heme iron enzymes, see refs 1, 4, 6, 80−84.

2. Nitrile Hydratase (NHase)

2.1. Enzyme Function

Nitrile hydratases(NHases) convert nitriles to less toxic amides cleanly and rapidly under mild conditions.[17,18,21−23,47,48,52,75,85−91] It has been proposed that nitriles serve as the sole carbon and/or nitrogen source for the growth of bacterial-containing NHase enzymes. NHases are found in microorganisms such as *Rhodococcus sp*. R312 and N771 and *Pseudomona chlorophis*.[28,92] Potential applications for this biocatalyst include the industrial production of amides,[93] enantioselective amide synthesis,[88] and conversion of nitrile wastes to less toxic amides. In Japan, microbial NHase is currently being used in the kiloton production of acrylamide.[93] In contrast to most hydrolytic enzymes, NHase contains iron, or in some cases cobalt,[19,94] as opposed to zinc.[95] The cobalt form of NHase (Co-NHase; vide infra) is utilized in industrial acrylamide production, because it is more stable than Fe-NHase. Zinc is usually the metal of choice for promoting biological hydrolytic reactions,[95,96] presumably because it is not complicated by redox chemistry. Iron, on the other hand, can promote unwanted side reactions with dioxygen (i.e., Fenton chemistry involving $OH^{\bullet}$ radicals) involving indiscriminant H-atom abstraction reactions resulting in damaged proteins or DNA.[97] For Fenton chemistry to occur, the 2+ oxidation state must be accessible,[98] however. The most extensively studied NHases are the Fe-NHases from *Rhodococcus sp*. R312 and N771.[18,21−23,26,28,48,92,99] Co-NHases are EPR silent,[19,94,100,101] and thus the active site is more difficult to probe spectroscopically.

2.2. Enzyme Active Site Structure

As described in the Introduction, the iron ion of NHase is ligated by an apical cysteinate sulfur (trans to the inhibitor/substrate binding site), two peptide amides, and two cysteinate sulfurs in the equatorial plane (Figure 1C). The N_2S_2 equatorial plane of this site looks very similar to that of the Ni^{2+} ion of acetyl-CoA synthase (ACS).[50] With NHase, the two

BATCH: cr80a25 USER: slr69 DIV: @xyv04/data1/CLS_pj/GRP_cr/JOB_i80/DIV_cr020619e DATE: January 2, 2004

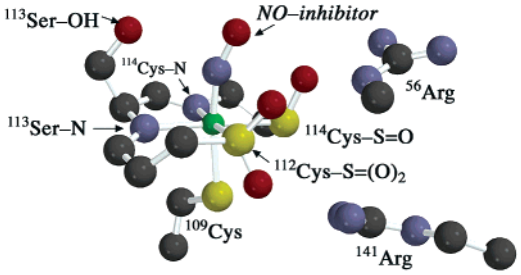

Figure 4. Active site of NO-inhibited nitrile hydratase (NHase).

cysteinate sulfurs in the equatorial plane appear to be oxygenated (i.e., post-translationally modified),[26,92,99,102] however, one to a sulfenate (^{114}Cys-S=(O)) and the other to a sulfinate (^{112}Cys-S=(O)$_2$; Figure 4). It is not clear whether both of these oxidized sulfurs are required for catalytic activity.[102] Dioxygen is required for activity when the recombinant unmodified protein lacking Fe is reconstituted with ferric citrate in a mercaptoethanol buffer. Since excess mercaptoethanol would reduce ferric citrate to ferrous citrate, it is not clear whether oxygen is required in order to oxidize the metal ion, the ligated cysteinates, or both.[99] The sulfinate is reproducibly observed in digested protein by mass spectroscopy, but the sulfenate is not.[28,102] Free sulfenates are unstable, however.[103] It is possible that the oxygens on the sulfurs are introduced during the digestion process. However, there does appear to be some correlation between activity and the amount of ^{112}-Cys-S=(O)$_2$ present.[99] Further oxygenation of the singly oxygenated ^{114}Cys-S=(O) apparently shuts down activity.[104] Definitive proof for the requirement of both oxygenated sulfurs would involve the correlation of enzyme activity with either the presence of $\nu_{S=O}$ stretches in the resonance Raman (RR) spectrum or the observation of oxygenated sulfurs by S-XAS. Studies of this nature have yet to be reported.

The NHase active site iron resides in a rather electron rich environment, given that five anionic ligands (two deprotonated amides and three cysteinates) ligate the iron.[26] Oxidation of one or two of the coordinated sulfur ligands would serve to remove some of this excess electron density. Tautomerization of the coordinated amides to their imidate form would also provide a mechanism for the removal of excess electron density from the iron. DFT calculations show that there is significant double-bond character between the nitrogen and carbon atoms of the coordinated peptide amides, implying that they have significant imidate character.[105] Two highly conserved arginines (Arg^{56}, Arg^{141}; Figure 4)[28,106] residing in the active site cavity (~5.0 Å away from the Fe) may also serve to remove some of this electron density. As shown in Figure 4, both Arg^{141} and Arg^{56} are within H-bonding distance of the sulfinate and sulfenate oxygens (^{112}Cys-S=(O)$_2$ and ^{114}Cys-S=(O)). Both of these arginines are required for catalytic activity.[28,106] It is also possible that the arginine closest to the "substrate" binding site (^{56}Arg) helps to stabilize a critical transition state or protonate an intermediate. A highly conserved serine hydroxyl group, ^{113}Ser-OH, also sits near[28,102] the "substrate binding site" (3.8 Å away from the Fe). It has been proposed that this serine-OH helps to stabilize the Fe(III)−NO species in NO-inhibited NHase by forming a "claw", along with the sulfinate and sulfenate oxygens (Figure 4), that holds NO in place.[26] Alternatively, this serine-OH may get involved in the catalytic cycle by either stabilizing a critical transition state or protonating intermediates along the reaction pathway.

2.3. Spectroscopic Properties

The Fe-NHase active site is characterized by an intense charge-transfer band near 700 nm in the electronic absorption spectrum (Table 1).[21,52,85] This intense band has been assigned as a sulfur-to-iron charge-transfer band on the basis of resonance enhancement of ν_{Fe-S} stretches in the RR spectrum.[23] The iron ion of NHase is in the 3+ oxidation state, low-spin ($S = {}^1/_2$), and redox inactive. The inability of this site to undergo redox reactions prevents unwanted Fenton or H-atom abstraction chemistry from occurring. The low spin-state of the NHase iron site is unusual for non-heme iron and unexpected, given the π-donor properties of the cysteinate thiolate ligands. The higher 3+ oxidation state of this site is uncommon, since transition-metal thiolates are prone to undergo autoreduction.[107−109] Dithiothreitol, a common biological reductant, does not reduce the Fe^{III} ion of NHase, however, indicating that the 3+ oxidation state is extremely stable in this enzyme.[85] The EPR signal associated with NHase is characteristic of an $S = {}^1/_2$ system containing an odd electron in a d_{xy} orbital.[23] The $g_{max} = 2.27$ associated with this EPR signal (Table 2) is low relative to, for example, the heme enzyme cytochrome P450 ($g_{max} = 2.45$),[110] suggesting that unpaired spin density is delocalized onto the ligating atoms of NHase. Both the UV/vis spectrum and the EPR signal of NHase are pH-, substrate-, and inhibitor-dependent (Tables 1 and 2).[22,23,52] This suggests that substrates (RCN) and inhibitors (N_3^-, NO, butyrate) bind to, or near, the metal site. The pH dependence has been attributed to the protonation of either a coordinated ligand or a nearby residue involved in H-bonding to one of the coordinated sulfurs (at pH = 7.3).[22,23] Enzyme activity is also pH-dependent; the pH = 9 form is inactive, whereas the pH = 7.3 form is active.[18]

2.4. NO Regulation of Activity

When whole-cell samples of NHase are stored in the dark at low temperatures, NHase is inactivated. Light exposure reactivates the enzyme.[48,86,87,89,90] Purified, isolated samples of the NHase enzyme, on the other hand, are not inactivated by the exclusion of light, implying that the source of inactivation is contained somewhere in the whole cells. This was ultimately proven to be the case when it was demonstrated that nitric oxide (NO$^\bullet$), produced by NO synthase, was responsible for the observed dark inactivation.[17,48,90,111] Upon the addition of authentic samples of NO$^\bullet$ (an $S = {}^1/_2$ radical), the $S = {}^1/_2$ EPR signal associated with NHase disappears,[48] and an IR stretch appears at 1853 cm^{-1}.[90] These observations

BATCH: cr80a25 USER: slr69 DIV: @xyv04/data1/CLS_pj/GRP_cr/JOB_i80/DIV_cr020619e DATE: January 2, 2004

Table 1. Comparison of Electronic Spectral Data for Nitrile Hydratase Enzyme vs Model Compounds

	$\lambda_{max}(\epsilon)$	
	aprotic solvent	H_2O
inactive enzyme (pH = 9)[a,b]		690(~1200)
active enzyme (pH = 7.3)[a,b]		710(~1200)
active enzyme (butyrate-free)[c]		676(NR)
enzyme + CH_3CH_2CN[d]		690(~4200)
[LFe^{III}] (**1**)[e]		651(6110), 775(4520)
[L^2Fe^{III}] (**2**)[e]		520(sh), 551(2370)
[$Fe^{III}(ADIT)_2$]$^+$ (**3**)[f]	718(1400)[#]	693(1400)
[$Fe^{III}(AMIT)_2$]$^+$ (**4**)[f,g]	696(1100)[#]	*g*
[$Fe^{III}(DITpy)_2$]$^+$ (**5**)[h]	784(1300)[#]	732(1400)
[$Fe^{III}(DITIm)_2$]$^+$ (**6**)[h]	802(1300)[#]	740(1200)
[$Fe^{III}(PyPepS)_2$]$^-$ (**7**)[i]	850(1900)[#]	
[$Fe^{III}(PyPepSO_2)_2$]$^-$ (**8**)[j]	~690(NR)[@]	~690(NR)
[$Fe^{III}(PyPS)$]$^-$ (**13**)[k]	540(3600), 650(3700)	
[$Fe^{III}(PyP\{SO_2\})$]$^-$ (**15**)[k]	360(5500), 480(3400)[@]	
[$Fe^{III}(PyP\{SO_2\})(CN)$]$^-$ [k]	640(1350)[@]	
[FeL_2*]$^+$	750(600), 1005(1410)[l]	
[$Fe^{III}(S_2{}^{Me_2}N_3(Pr,Pr))$]$^+$ (**25**)[m]	416(4200)	*g*
[$Fe^{III}(S_2{}^{Me_2}N_3(Pr,Pr))(N_3)$] (**27**)[m]	708(1600)	*g*
[$Fe^{III}(S_2{}^{Me_2}N_3(Et,Pr))$]$^+$ (**38**)[n]	493(1530), 532(1520)	*g*
[$Fe^{III}(S_2{}^{Me_2}N_3(Et,Pr))(MeCN)$]$^+$ (**39**)[o]	833(840)	*g*
[$Fe^{III}(PyPS)(N\text{-}MeIm)$]$^-$ [p]	910(1600), 700(1800)[@]	
[$Fe^{III}(PyPSO_2)(CN)$]$^{2-}$ [p]	470(1600), 640(1350)	
[$Fe^{III}(PyPSO_2)(CN)$]$^{2-}$ [p]	425(1800), 660(1200)	
[$Fe^{III}(PyPS)(MeOH)$]$^-$	550(3800), 790(950)	
[$Fe^{III}(PyPS)(OH)$]$^{2-}$ (**36**)[p]	595(3900), 790(700)	

[a] These spectra were recorded in the presence of a butyrate buffer. [b] Brennan, B. A.; Cummings, J. G.; Chase, D. B.; Turner, I. M., Jr.; Nelson, M. J. *Biochemistry* **1996**, *35*, 10068. [c] Honda, J.; Kandori, H.; Okada, T.; Nagamune, T.; Shichida, Y.; Sasabe, H.; Endo, I. *Biochemistry* **1994**, *33*, 3577. [d] Sugiura, Y.; Kuwahara, J.; Nagasawa, T.; Yamada, H. *J. Am. Chem. Soc.* **1987**, *109*, 5848. [e] Beissel, T.; Buerger, K. S.; Voigt, G.; Wieghardt, K.; Butzlaff, C.; Trautwein, A. X. *Inorg. Chem.* **1993**, *32*, 124. [f] Shoner, S. C.; Barnhart, D.; Kovacs, J. A. *Inorg. Chem.* **1995**, *34*, 4517. [g] Unstable in aqueous solutions. [h] Jackson, H. L.; Shoner, S. C.; Rittenberg, D.; Cowen, J. A.; Lovell, S.; Barnhart, D.; Kovacs, J. A. *Inorg. Chem.* **2001**, *40*, 1646. [i] Noveron, J. C.; Olmstead, M. M.; Mascharak, P. K. *Inorg. Chem.* **1998**, *37*, 1138. [j] Tyler, L. A.; Noveron, J. C.; Olmstead, M. M.; Mascharak, P. K. *Inorg. Chem.* **1999**, *38*, 616. [k] Noveron, J. C.; Olmstead, M. M.; Mascharak, P. K. *J. Am. Chem. Soc.* **2001**, *123*, 3247. [l] Nivorozhkin, A. L.; Uraev, A. I.; Bondarenko, G. I.; Antsyshkina, A. S.; Kurbatov, V. P.; Garnovskii, A. D.; Turta, C. I.; Brashoveanu, N. D. *J. Chem. Soc., Chem Commun.* **1997**, 1711. L* = 5-mercapto-1-phenyl-3-methyl-4-ylmethylene(8-amino)-quinoline. [m] Ellison, J. J.; Nienstedt, A.; Shoner, S. C.; Barnhart, D.; Cowen, J. A.; Kovacs, J. A. *J. Am. Chem. Soc.* **1998**, *120*, 5691. [n] Schweitzer, D.; Shearer, J.; Rittenberg, D. K.; Shoner, S. C.; Ellison, J. J.; Loloee, R.; Lovell, S.; Barnhart, D.; Kovacs, J. A. *Inorg. Che*m. **2002**, *41*, 3128. [o] Shearer, J.; Jackson, H. L.; Schweitzer, D.; Rittenberg, D. K.; Leavy, T. M.; Kaminsky, W.; Scarrow, R. C.; Kovacs, J. A. *J. Am. Chem. Soc.* **2002**, *124*, 11417. [p] Noveron, J. C.; Olmstead, M. M.; Mascharak, P. K. *J. Am. Chem. Soc.* **2001**, *123*, 3247. [#]Spectrum in MeCN. NR = not reported. [@]Spectrum in DMF.

indicate that NO binds to the metal site, and that once bound it looks more like NO$^\bullet$ than NO^+ or NO^-. Nitric oxide (NO) apparently displaces the H_2O/OH^- and thereby prevents nitriles from binding to the metal ion, or replaces the catalytically active Fe−OH species (vide infra). Light photolytically cleaves the Fe−NO bond by promoting an electron into an orbital with σ*(Fe−NO) character, resulting in the release of NO$^\bullet$.[17] Density functional calculations show that an orbital with σ*(Fe−NO) character lies near the filled NO-character orbitals, making this mechanism of Fe−NO bond cleavage feasible.[112] Once NO is released, the coordinatively unsaturated metal ion would be more accessible to nitriles and/or water. Consistent with this possibility, Munck and Nelson have shown that a five-coordinate intermediate forms at low temperatures upon the release of NO, which then converts to the six coordinate hydroxide-bound form upon warming.[113] Nitric oxide appears, therefore, to play a regulatory role, in which it turns NHase activity off and on, depending on the light conditions, by binding to the Fe^{III} ion.[77]

2.5. Proposed Mechanism

Although the structure of NHase has been defined, a number of unresolved questions have yet to be adequately addressed. One of these concerns the mechanism of nitrile hydrolysis. Nitriles are extremely resistant to hydrolysis. The nitrile carbon atom is only very slightly electrophilic, making it unsusceptible to attack by water (or hydroxide) except under forcing conditions (at elevated temperatures). Rates are enhanced either by increasing the electrophilicity of the nitrile carbon or by using reagents more nucleophilic than hydroxide. Thiolates, for example, have been shown to catalyze nitrile hydrolysis via the formation of a thioimidate intermediate (Figure 5),[114] which is readily hydrolyzed.[115,116] In fact, nitrilase,[72,116] the enzyme that hydrolyzes nitriles all the way to the corresponding acid and ammonia, possesses a catalytic cysteinate and no metal ion. Mercaptoethanol will hydrolyze nitriles with ~10^3 rate enhancement vs the uncatalyzed rates.[115,116] This is ~10^{-3} slower than M^{3+}-catalyzed reactions (vide infra).[117] Under basic conditions (e.g., 0.65 M [OH^-]), reactions are first order in both nitrile and hydroxide, indicating that the transition state involves direct attack of hydroxide at the nitrile carbon. The reported activation energy for nitrile hydrolysis under these conditions is 20.3 kcal/mol.[118] In the presence of a Bronstead acid, E_a is ~5 kcal/mol higher than that of the base-promoted reaction

BATCH: cr80a25 USER: slr69 DIV: @xyv04/data1/CLS_pj/GRP_cr/JOB_i80/DIV_cr020619e DATE: January 2, 2004

Table 2. EPR Parameters for Synthetic Analogues vs Nitrile Hydratase

	g-values		
NHase enzyme (pH = 7.3)[a,b]	2.27	2.14	1.97
NHase enzyme (pH = 9)[a,b]	2.20	2.12	1.99
NHase enzyme + $(CH_3)_2CHCN$ (pH = 7.2)[a,c]	2.21	2.12	1.98
NHase enzyme + N_3^- [a,c]	2.23	2.14	1.99
NHase enzyme + NO[d]	EPR silent		
Fe(salen)(TGE(S^-)(H_2O)[e]	2.27	2.11	1.97
[LFe^{III}] (**1**)[f]	2.54	2.14	1.5
$[Fe(III)(ADIT)_2]^+$ (**3**)[g]	2.19	2.13	2.01
$[Fe(III)(AMIT)_2]^+$ (**4**)[g]	2.20	2.16	2.00
$[Fe(III)(DITpy)_2]^+$ (**5**)[h]	2.16	2.10	2.02
$[Fe(III)(DITIm)_2]^+$ (**6**)[h]	2.19	2.15	2.01
$[Fe(III)(PyPepS)_2]^-$ (**7**)[i]	2.22	2.14	1.98
$[Fe^{III}(Haetaln)_2]^+$ (**9**)[j]	2.16	2.12	2.00
$[Fe^{III}(PyPS)(N\text{-}MeIm)]^-$ [k]	2.32	2.15	1.93
$[Fe^{III}(PyPS)(OH)]^{2-}$ (**36**)[k]	2.31	2.12	1.93
[(bmmp-TASN)Fe^{III}CN][l]	2.31	2.16	1.96
$[Fe^{III}(S_2^{Me_2}N_3(Pr,Pr))]^+$ (**25**)[m]	2.15	2.07	2.00
$[Fe^{III}(S_2^{Me_2}N_3(Pr,Pr))(N_3)]$ (**27**)[m]	2.23	2.16	1.99
$[Fe^{III}(S_2^{Me_2}N_3(Pr,Pr))(NO)]^+$ (**26**)[n]	EPR silent		
[(bmmp-TASN)$Fe^{III}NO]^+$ [o]	EPR silent		
$[Fe^{III}(S_2^{Me_2}N_3(Et,Pr)]^+$ (**38**)[p]	2.12	2.07	2.02
$[Fe^{III}(S_2^{Me_2}N_3(Et,Pr))(MeCN)]^+$ (**39**)[p]	2.17	2.14	2.01

[a] These spectra were recorded in the presence of a butyrate buffer, which was added in order to stabilize the samples. Since butyrate appears to act as an inhibitor, the reported *g*-values are therefore those of a "butyrate-inhibited" form of the enzyme. [b] Brennan, B. A.; Cummings, J. G.; Chase, D. B.; Turner, I. M., Jr.; Nelson, M. J. *Biochemistry* **1996**, *35*, 10068. [c] Sugiura, Y.; Kuwahara, J.; Nagasawa, T.; Yamada, H. *J. Am. Chem. Soc.* **1987**, *109*, 5848. [d] Odaka, M.; Fujii, K.; Hoshino, M.; Noguchi, T.; Tsujimura, M.; Nagashima, S.; Yohada, N.; Nagamune, T.; Inoue, I.; Endo, I. *J. Am. Chem. Soc.* **1997**, *119*, 3785. [e] Sakurai, H.; Tsuchiya, K.; Migita, K.. *Inorg. Chem.* **1988**, *27*, 3879. [f] Beissel, T.; Buerger, K. S.; Voigt, G.; Wieghardt, K.; Butzlaff, C.; Trautwein, A. X. *Inorg. Chem.* **1993**, *32*, 124. [g] Shoner, S. C.; Barnhart, D.; Kovacs, J. A. *Inorg. Chem.* **1995**, *34*, 4517. [h] Jackson, H. L.; Shoner, S. C.; Rittenberg, D.; Cowen, J. A.; Lovell, S.; Barnhart, D.; Kovacs, J. A. *Inorg. Chem.* **2001**, *40*, 1646. [i] Noveron, J. C.; Olmstead, M. M.; Mascharak, P. K. *Inorg. Chem.* **1998**, *37*, 1138. [j] Marini, P. J.; Murray, K. S.; West, B. O. *J. Chem. Soc., Dalton Trans.* **1983**, 143. [k] Noveron, J. C.; Olmstead, M. M.; Mascharak, P. K. *J. Am. Chem. Soc.* **2001**, *123*, 3247. [l] Grapperhaus, C. A.; Li, M.; Patra, A. K.; Potuovic, S.; Kozlowski, P. M.; Zgierski, M. Z.; Mashuta, M. S. *Inorg. Chem.* **2003** *42*, 4382. [m] Ellison, J. J.; Nienstedt, A.; Shoner, S. C.; Barnhart, D.; Cowen, J. A.; Kovacs, J. A. *J. Am. Chem. Soc.* **1998**, *120*, 5691. [n] Schweitzer, D.; Ellison, J. J.; Shoner, S. C.; Lovell, S.; Kovacs, J. A. *J. Am. Chem. Soc.* **1998**, *120*, 10996. [o]Grapperhaus, C. A.; Patra, A. K.; Mashuta, M. S *Inorg. Chem.* **2002**, *41*, 1039. [p] Shearer, J.; Jackson, H. L.; Schweitzer, D.; Rittenberg, D. K.; Leavy, T. M.; Kaminsky, W.; Scarrow, R. C.; Kovacs, J. A. *J. Am. Chem. Soc.* **2002**, *124*, 11417.

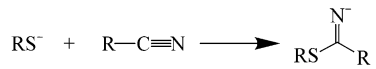

Figure 5. Possible mechanism of nitrile hydrolysis involving a cysteinate or thiolate to afford a readily hydrolyzed thioimidate intermediate.

and requires higher concentrations of acid (>11 M). The intermediate amide is hydrolyzed ~10 times faster than the nitrile substrate.[118] Consequently, free nitrile hydrolysis usually proceeds all the way to the carboxylic acid. Thiolate-catalyzed nitrile hydrolyses can be stopped at the amide by controlling the pH ($3 < pH < 8$).[115] Transition metals selectively catalyze hydrolysis of nitriles, stopping at the amide. Upon coordination to a Lewis acidic metal ion, the nitrile carbon atom is activated toward nucleophilic attack by OH^-, the activation barrier is lowered, and the developing imidate anion is stabilized.[119−121]

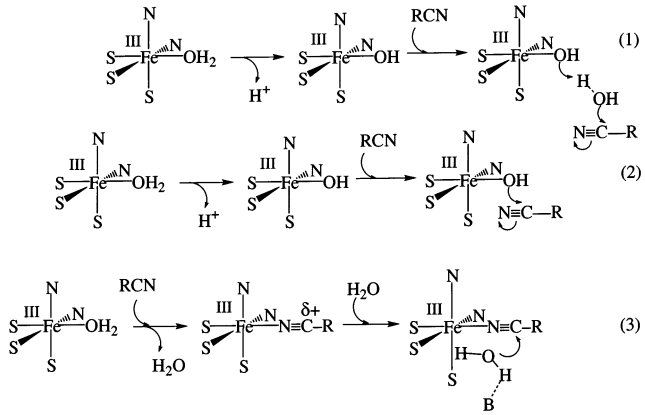

Figure 6. Proposed reaction mechanisms for nitrile hydrolysis by the metalloenzyme nitrile hydratase (NHase).

Nitrile hydratase hydrolyzes nitriles under mild conditions (pH = 7.5, ambient temperature). Assays for nitrile hydratase activity frequently use either propionitrile or methacrylonitrile (MAN) as substrates. The Michaelis−Menten constant K_m and V_{max} values for hydrolysis of MAN vary from $K_m = 1.95$ (*Rhodococcus sp.* N-771)[106] to 0.282 mM (*Rhodococcus sp.* YH3-3),[122] and from $V_{max} = 1600$ (*Rhodococcus sp.* N-771) to 287 μmol-product·min^{-1}·mg-$protein^{-1}$ (*Rhodococcus sp.* YH3-3), respectively. Reported K_m and V_{max} values for hydrolysis of propionitrile are 77.8 mM and 1280 μmol-product·min^{-1}·mg-$protein^{-1}$, respectively.[122] The reported activation energy for nitrile hydrolysis by NHase (from *Brevibacterium imperialis* CBS 489-74) is 13.75 kcal/mol.[123] Three distinct mechanisms of nitrile hydrolysis by NHase have been proposed (Figure 6).[25] It has also been proposed that the sulfenate sulfurs may be directly involved in the mechanism (vide infra).[69] Two of the mechanisms shown in Figure 6 (mechanisms 1 and 2) involve the metal ion generating a hydroxide source for the nucleophilic attack of a free nitrile, with (mechanism 1) or without (mechanism 2) the involvement of an intervening water molecule. The third (mechanism 3) is the only mechanism that would increase the nitrile carbon's electrophilicity via its coordination to the Lewis acidic metal ion. One could argue that the five anionic ligands make the Fe^{3+} ion of NHase a poor Lewis acid; however, the oxygenated sulfurs[26,99,102] and nearby H-bonded residues (e.g., Arg, Figure 4)[28,106] would offset this. The fact that the pK_a of a M^{3+}-bound water has been shown to decrease upon oxygenation of a thiolate (in an NHase model complex) supports this possibility.[124] Also consistent with this, recent DFT calculations indicate that the iron ion of NHase is modestly positively charged (calculated Mulliken charge = +0.49),[112] supporting its possible role as a Lewis acid. The last two mechanisms shown in Figure 6 are differentiated from the first in that they involve metal-bound intermediates and require that the metal ion release product at reasonably fast rates. One might predict, however, that this would be problematic for "substitution inert" low-spin Co(III) and low-spin Fe(III).[125,126] There is spectroscopic evidence that supports mechanism 3, however.[52] Both

BATCH: cr80a25 USER: slr69 DIV: @xyv04/data1/CLS_pj/GRP_cr/JOB_i80/DIV_cr020619e DATE: January 2, 2004

the EPR signal and electronic absorption spectrum of NHase change upon the introduction of nitriles.[52] One could interpret this to mean that nitriles coordinate to the metal ion; however, it is also possible that the nitrile indirectly perturbs the metal ion by slightly distorting its structure as it "wedges" itself in the active site pocket. There is also literature precedent for mechanism 3.[117,127,128] Metal ions have been shown to enhance nitrile hydrolysis rates by as much as 10^6-10^7, and rate enhancement is greater for 3+ vs 2+ metal ions (vide infra).[117,127] Mechanism 1 resembles that by which Zn(II) hydrolytic enzymes operate.[129−131] Zn^{II}-containing hydrolytic enzymes typically hydrolyze more electrophilic substrates, requiring less activation. Peptide deformylase hydrolyzes more electrophilic substrates, which might explain why it contains a lower valent Fe^{II} ion,[46] as opposed to Fe^{III}. Why PDF contains Fe^{II} rather than Zn^{II} is not understood.[44,46] There had been some controversy surrounding the identity of the metal ion in the active PDF catalyst,[44] and some originally believed Zn^{II} to be the active catalyst.[43] Although one would not expect a hydroxide coordinated to a 3+ metal ion to be a good nucleophile, the large number of anionic ligands coordinated to the Fe(III) ion would partially decrease the metal ion's "3+ charge". As described by Caulton,[132] it is likely that the HOMO of an M−OH contains a rather large lobe concentrated on the distal side of the O-atom, making it a better nucleophile than free OH^-.

2.6. Cobalt-NHase

Cobalt(III) replaces Fe(III) in NHases obtained from *Pseudomonas putida, Rhodococcus rhodochrous* J1, and *Pseudonocardia thermophila*.[19,94,133−135] Like the iron enzyme, the cobalt enzyme is redox inactive and low-spin ($S = 0$). Low-spin Co(III) is very rarely utilized in metalloenzymes, in part because it is extremely inert with respect to substitution reactions.[136] This begs the question: *How can nature utilize a substitution-inert metal ion? Does this imply something about the mechanism?* Perhaps it suggests that substrates do not actually bind to the metal center. Or, perhaps nature has devised some way around this problem. The large amount of sequence homology in the active site regions of Fe-NHase and Co-NHase foretold their nearly identical structures, as revealed by X-ray crystallography.[101] This structural similarity was also anticipated on the basis of experiments which showed that replacement of the Fe^{3+} ion of Fe-NHase from *Rhodococcus* sp. n-771 with Co^{3+} resulted in an enzyme with properties identical to those of Co-NHase from *Pseudomonas putida* NRRL-18668.[133] Co-NHases are more stable than Fe-NHases and preferentially react with aromatic nitriles, in contrast to the Fe-NHases which preferentially react with aliphatic nitriles. Differences in conserved residues located in the α-subunit, and thought to be involved in substrate recognition and binding, are most likely responsible for these differences. Nitric oxide (NO) does not appear to coordinate to the metal ion of Co-NHase. Since it contains a low-spin d^6 ($S = 0$) Co^{3+} ion (a weakly colored EPR-silent metal ion), Co-NHase has been more difficult to probe spectroscopically than Fe-NHase. Thus, very little spectroscopic data is available on this subclass of NHases.

2.7. Electronic and Geometric Structural Models of NHase

The molecular-level details regarding metalloprotein function emerge from several complementary lines of study, at the interface of chemistry, biology, and physics.[137,138] Protein structure and function can be probed using high-resolution (synchrotron) X-ray crystallography and site-directed mutagenesis. Application of biophysical techniques (such as EXAFS, RR, MCD, EPR, ENDOR, and Mossbauer) which specifically probe the metal ion and its surroundings reveals details about the electronic and geometric structure of the active site.[5,139−142] Systematic alteration of the active site structure allows one to correlate structure with properties and function. This is readily accomplished with synthetic models.[143] Small molecular analogues reproducing key spectroscopic features help to fine-tune details regarding active site structure and mechanism by providing, for example, parameters needed to interpret biophysical data. Details regarding key bond lengths (e.g., the O−O distance of an activated O_2 intermediate), the presence or absence of protons,[144−147] or the identity of intermediates can be "fuzzy" or lacking, due to limitations imposed by either the biological system or the physical technique. Quite often these details can be revealed via synthetic models.

2.7.1. The Influence of Thiolates and Amides on Properties

Monomeric thiolate-ligated Fe^{III} complexes are difficult to synthesize, due to the electron-rich nature of the ligand, which favors autoreduction of the metal.[108] The additional lone pairs of the thiolate ligand can be used either to form multiple bonds to a single metal ion or, more commonly, to form bridges to other metals.[148,149] Consequently, dimeric or polymeric structures frequently form as the predominant product in reactions between thiolates and metal ions. Steric bulk is usually required to avoid these undesirable reaction pathways.[108] Reactions with oxidants such as superoxide and peroxide are complicated by the potential for initial attack at, and ultimate oxidation of, the sulfur rather than the metal ion. Despite these synthetic challenges, much progress has been made in the biomimetic modeling of cysteinate-ligated non-heme iron active sites in biology.[54,63−65,69,124−126,150−165]

The first attempt at modeling NHase was reported in 1988 by Sakurai.[166] In this study, ethyl thioglycolate (TGE) was added to $[Fe^{III}(salen)]^+$ ($g = 4.3$) in an EPR tube, resulting in the appearance of a new low-spin Fe^{III} signal with $g = 2.284$, 2.110, and 1.972 (Table 2). Further characterization of this low-spin species was never reported. In 1993, Wieghardt reported a six-coordinate tris-thiolate-ligated Fe^{III} complex, $[LFe^{III}]$ (**1**; Figure 7, L = 1,4,7-tris(4-*tert*-butyl-2-mercaptobenzyl)-1,4,7-triazacyclononane),[156] which is intensely colored and low-spin ($S = {}^1/_2$) at low temperatures (Table 2). A thermally accessible $S =$

BATCH: cr80a25 USER: slr69 DIV: @xyv04/data1/CLS_pj/GRP_cr/JOB_i80/DIV_cr020619e DATE: January 2, 2004

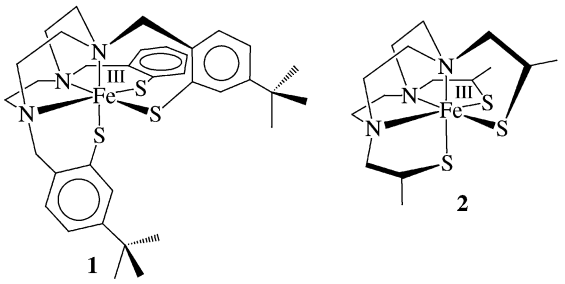

Figure 7. Wieghardt's NHase models [LFe^{III}] (**1**; L = 1,4,7-tris(4-*tert*-butyl-2-mercaptobenzyl)-1,4,7-triazacyclononane) and [L^{2}Fe^{III}] (**2**, L^2 = 1,4,7-tris(2-mercaptopropyl)-1,4,7-triazacyclononane).

Table 3. Iron−Sulfur Bond Lengths in Synthetic Analogues for the Low-Spin, Thiolate-Ligated, Non-Heme Fe^{III} Site of Nitrile Hydratase

model complex	average Fe−S bond length (Å)
[LFe^{III}] (**1**)[a]	2.28(1)
[Fe^{III}(ADIT)$_2$]$^+$ (**3**)[b]	2.203(4)
[Fe^{III}(AMIT)$_2$]$^+$ (**4**)[c]	2.232(2)
[Fe^{III}(DITpy)$_2$]$^+$ (**5**)[c]	2.19(1)
[Fe^{III}(DITIm)$_2$]$^+$ (**6**)[c]	2.211(2)
[Fe^{III}(PyPepS)$_2$]$^-$ (**7**)[d]	2.229(1)
[Fe^{III}(PyPepSO$_2$)$_2$]$^-$ (**8**)[e]	2.21(2)
[FeL$_2$*]$^+$ [f]	2.23(1)
[Fe^{III}(Haetaln)$_2$]$^+$ (**9**)[g]	2.21(1)
[Fe^{III}(S$_2$^{Me_2}N$_3$(Pr,Pr))(N$_3$)] (**28**)[h]	2.20(1)

[a] Beissel, T.; Buerger, K. S.; Voigt, G.; Wieghardt, K.; Butzlaff, C.; Trautwein, A. X. *Inorg. Chem.* **1993**, *32*, 124. [b] Shoner, S. C.; Barnhart, D.; Kovacs, J. A. *Inorg. Chem.* **1995**, *34*, 4517. [c] Jackson, H. L.; Shoner, S. C.; Rittenberg, D.; Cowen, J. A.; Lovell, S.; Barnhart, D.; Kovacs, J. A. *Inorg. Chem.* **2001**, *40*, 1646. [d] Noveron, J. C.; Olmstead, M. M.; Mascharak, P. K. *Inorg. Chem.* **1998**, *37*, 1138. [e] Tyler, L. A.; Noveron, J. C.; Olmstead, M. M.; Mascharak, P. K. *Inorg. Chem.* **1999**, *38*, 616. [f] Nivorozhkin, A. L.; Uraev, A. I.; Bondarenko, G. I.; Antsyshkina, A. S.; Kurbatov, V. P.; Garnovskii, A. D.; Turta, C. I.; Brashoveanu, N. D. *J. Chem. Soc., Chem Commun.* **1997**, 1711. L* = 5-mercapto-1-phenyl-3-methyl-4-ylmethylene(8-amino)quinoline. [g] Fallon, G. D.; Gatehouse, B. M. *J. Chem. Soc., Dalton Trans.* **1975**, 1344. [h] Ellison, J. J.; Nienstedt, A.; Shoner, S. C.; Barnhart, D.; Cowen, J. A.; Kovacs, J. A. *J. Am. Chem. Soc.* **1998**, *120*, 5691.

$^5/_2$ state results in an $S = {}^1/_2 \leftrightarrow S = {}^5/_2$ spin-equilibrium and slightly longer Fe−S bond lengths (2.28 Å) in **1** relative to those reported (2.21 Å) for NHase (Table 3). The electronic spectrum of **1** is dominated by two intense charge-transfer bands at 651(6110) and 775(4520) nm (Table 1). When the phenyl thiolates of **1** (Figure 6) are replaced with more-electron-donating alkanethiolates, the $S = {}^5/_2$ state in the resulting complex [L^{2}Fe^{III}] (**2**, L^2= 1,4,7-tris(2-mercaptopropyl)-1,4,7-triazacyclononane) is stabilized relative to the $S = {}^1/_2$ state, and the charge-transfer band shifts to 551(2370) nm (Table 1). In 1995, Kovacs showed that when two *cis*-alkanethiolates and two imines are incorporated into the coordination sphere, the spectroscopic and magnetic properties (electronic spectrum (Figure 8) and EPR (Figure 10), $S = {}^1/_2$) of the resulting model complexes ([Fe^{III}(ADIT)$_2$]$^+$ (**3**) and [Fe^{III}(AMIT)$_2$]$^+$ (**4**); Figure 9) closely resemble those of the NHase enzyme (Tables 1 and 2).[63] As shown in Figure 8, the electronic spectrum of **3** is remarkably similar to that of the NHase enzyme,[63] with an intense low-energy band

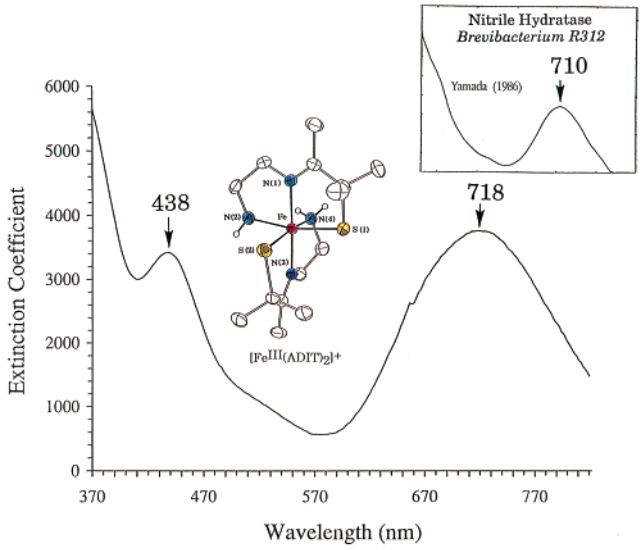

Figure 8. Electronic absorption spectrum of model complex [Fe^{III}(ADIT)$_2$]$^+$ (**3**) vs that of the NHase enzyme.

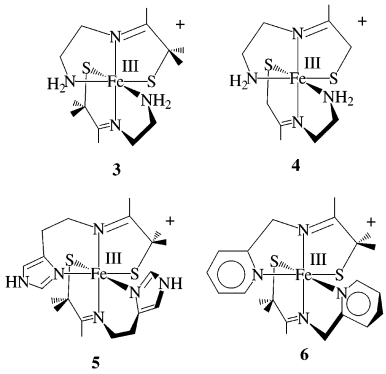

Figure 9. Kovacs's NHase models [Fe^{III}(ADIT)$_2$]$^+$ (**3**), [Fe^{III}(AMIT)$_2$]$^+$ (**4**), [Fe^{III}(DITIm)$_2$]$^+$ (**5**), and [Fe^{III}(DITpy)$_2$]$^+$ (**6**).

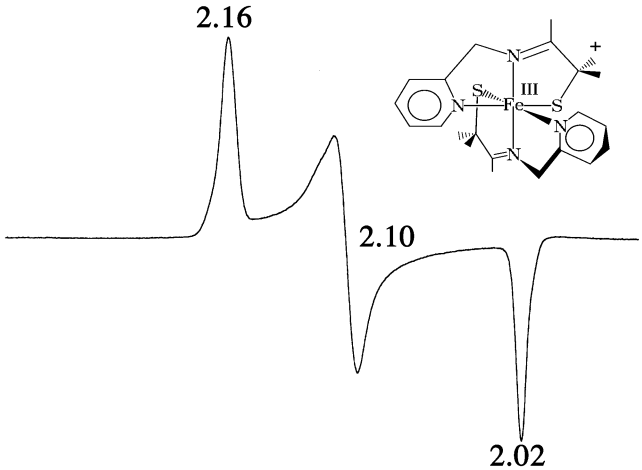

Figure 10. X-band EPR spectrum of [Fe^{III}(DITpy)$_2$]$^+$ (**6**).

assigned[167] (for a model closely related to **3**) as a πS-to-Fe charge transfer in character. This low-energy band is consistently observed as long as two *cis*-thiolates and imines (Me−C=N−) are included in the primary coordination sphere (Table 1).[64] Replacement of the terminal amines of **3** with imidazoles (**5**) or pyridines (**6**; Figure 9) only slightly perturbs the electronic absorption spectrum, and the spin-state

BATCH: cr80a25 USER: slr69 DIV: @xyv04/data1/CLS_pj/GRP_cr/JOB_i80/DIV_cr020619e DATE: January 2, 2004

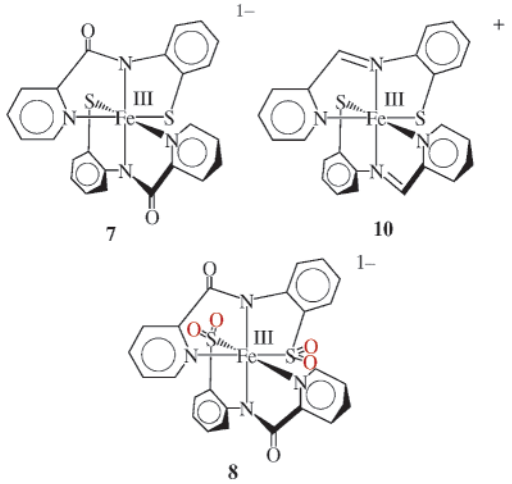

Figure 11. Mascharak's carboxamide-ligated $[Fe^{III}(PyPepS)_2]^-$ (**7**), imine-ligated $[Fe^{III}(PyAS)_2]^+$ (**10**), and sulfinate-ligated $[M^{III}(PyPepSO_2)_2]^-$ (M^{III} = Fe (**8**) and Co (**11**)) NHase model complexes.

remains $S = {}^1/_2$ (Tables 1 and 2).[64] *gem*-Dimethyl substitutents adjacent to the sulfurs add both thermodynamic stability and steric protection, preventing dimerization.[64] Removal of these methyls results in a less stable complex ($[Fe^{III}(AMIT)_2]^+$ (**4**; Figure 9)) with longer Fe^{III}–S bonds (Table 3). In 1999, Mascharak showed that when imines are replaced with amides in aromatic Fe^{III}–thiolate complexes, the electronic spectral properties of the resulting complex (Table 1) most closely resemble those of the NHase enzyme after oxygens are added to the sulfurs.[158] Addition of two oxygens to each of the aromatic thiolate sulfurs of $[Fe^{III}(PyPepS)_2]^-$ (**7**, Figure 11),[54] to afford $[Fe^{III}(PyPepSO_2)_2]^-$ (**8**), causes a color change from red to green, and the lower-energy band (Table 1) at ~850 nm shifts to ~690 nm (closer to that of the NHase enzyme).[158]

From the intensity of the low-energy electronic absorption bands associated with **3**–**6** (Table 1), it is clear that the Fe–S bonds in these complexes are fairly covalent, but not quite as covalent as, say, the Cu–S cysteinate bonds found in blue copper proteins (ϵ = 3000–5000).[168] The high degree of covalency in the Fe–S bonds of model compounds **1**,[156] **3**–**6**,[63,64] **7**,[54] and **8**[158] is reflected in their extremely short Fe–S bonds (Table 3) and low spin-state (Table 2). Prior to the synthesis of $[Fe^{III}(ADIT)_2]^+$ (**3**),[63] the only other example of an Fe^{III}–thiolate with distances as short as 2.2 Å was $[Fe^{III}(Haetaln)_2]^+$ (**9**), which was reported in 1975 by Gatehouse.[169] The delocalization of electrons within these covalent bonds reduces the energy required to pair electrons (the nephelauxetic effect), allowing easy access to the low spin-state.[170] With compounds **3**–**6**, the involvement of only one (d_{xy}) as opposed to three (the entire t_{2g} set) π-symmetry d orbitals also contributes to the low spin-state.[167] Thiolate-ligated $[Fe^{III}(ADIT)_2]^+$ (**3**),[63] $[Fe^{III}(PyPepS)_2]^-$ (**7**),[54] and $[Fe^{III}(PyPepSO_2)_2]^-$ (**8**)[158] are all low-spin ($S = {}^1/_2$), indicating that even in the absence of anionic amides, aliphatic thiolates alone will favor a low spin-state (Table 2). Imine-ligated **3** is low-spin even at ambient temperature, with no signs of thermally accessible higher spin-states.[63]

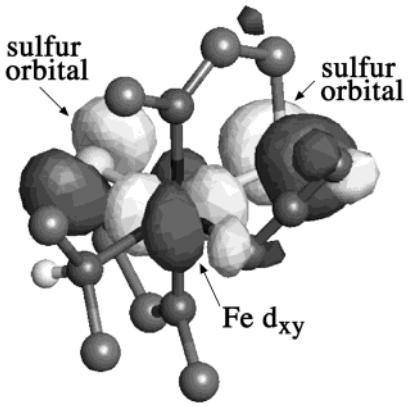

Figure 12. SOMO (singly occupied molecular orbital) of the NHase model $[Fe^{III}(S_2{}^{Me_2}N_3(Pr,Pr))(N_3)]$ (**28**).

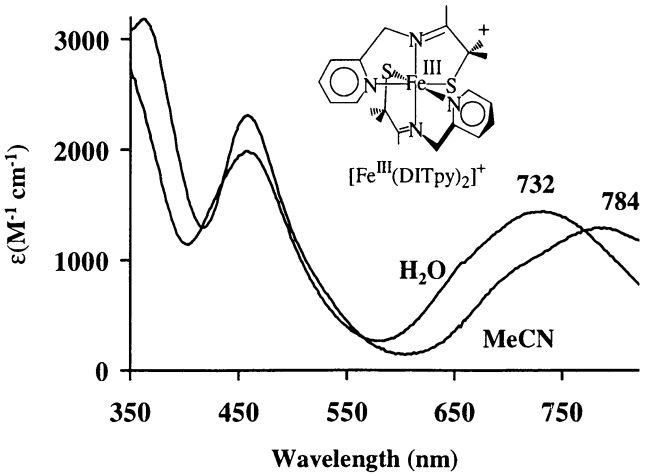

Figure 13. Electronic absorption spectrum of $[Fe^{III}(DITpy)_2]^+$ (**6**) in aprotic (MeCN) vs protic (H_2O) solvents, showing the blue shift that occurs upon H-bonding.

Oxygenation of the sulfurs has very little effect on the preferred spin-state as long as deprotonated amides are included in the coordination sphere.[158] The fairly narrow *g*-spread ($\Delta g = g_{max} - g_{min} = 0.14$; Table 2) in the rhombic EPR spectra of these complexes (as illustrated for **6** in Figure 10) supports the notion that there is extensive mixing of ligand orbital character into the singly occupied MO. Most $S = {}^1/_2$ systems, including cytochrome P450 (g = 2.45, 2.26, and 1.91),[51,67] have a larger *g*-spread than is seen with complexes **3**–**6**. Delocalization of electrons within the highest occupied molecular orbital of **3** is also supported by Kennepohl and Solomon's density function calculations on a related model.[167] These calculations show that the SOMO (singly occupied molecular orbital) d_{xy}(Fe–Sπ*) of **3** has significant sulfur character (Figure 12).

The S$\pi \rightarrow$ Fe(III) CT absorption band associated with low-spin Fe^{III}–thiolate complexes **3**–**6** (Figures 9) is a sensitive reporter of perturbations to not only the primary coordination sphere but also the outer coordination sphere, (i.e., the ligand's periphery, as well as solvent). Complexes **3**–**6** are all soluble in water as well as most organic solvents. As the H-bonding ability of the solvent is increased (Table 1), the CT band blue-shifts (Figure 13).[64] This shift is what one would expect if the sulfurs were involved in H-bonding to the solvent (Figure 14). H-bonding

Table 4. Redox Potentials ($E_{1/2}$ vs SCE) of Model Compounds vs Nitrile Hydratase

	DMF		CH_3CN		H_2O	
	$E_{1/2}$ (V)	ΔE (mV)	$E_{1/2}$ (V)	ΔE (mV)	$E_{1/2}$ (V)	ΔE (mV)
$[LFe^{III}]$ (**1**)[a]	−0.60[@]	NR				
$[L^2Fe^{III}]$ (**2**)[a]	−1.16[@]	NR				
$[Fe(III)(ADIT)_2]^+$ (**3**)[b]			−1.02	90	−0.77	60
$[Fe(III)(AMIT)_2]^+$ (**4**)[b]			−0.86	90		
$[Fe(III)(DITpy)_2]^+$ (**5**)[b]			−0.93	90	−0.74	60
$[Fe(III)(DITIm)_2]^+$ (**6**)[b]			−0.68	350		
$[Fe(III)(PyPepS)_2]^-$ (**7**)[c]	−1.12	120				
$[Fe(III)(PyAS)_2]^+$ (**10**)[d]	−0.13	60				
$[Fe(III)(PyMS)_2]^+$ [d]	−0.51	NR[f]				
$[(bmmp\text{-}TASN)Fe^{III}CN]$[e]	−0.88					
NHase enzyme[g,h]					−0.48	NR[f]

[a] Beissel, T.; Buerger, K. S.; Voigt, G.; Wieghardt, K.; Butzlaff, C.; Trautwein, A. X. *Inorg. Chem.* **1993**, *32*, 124. [b] Jackson, H. L.; Shoner, S. C.; Rittenberg, D.; Cowen, J. A.; Lovell, S.; Barnhart, D.; Kovacs, J. A. *Inorg. Chem.* **2001**, *40*, 1646. [c] Noveron, J. C.; Olmstead, M. M.; Mascharak, P. K. *Inorg. Chem.* **1998**, *37*, 1138. [d] Noveron, J. C.; Herradora, R.; Olmstead, M. M.; Mascharak, P. K. *Inorg. Chim. Acta.* **1999**, *285*, 269. [e] Grapperhaus, C. A.; Li, M.; Patra, A. K.; Potuovic, S.; Kozlowski, P. M.; Zgierski, M. Z.; Mashuta, M. S. *Inorg. Chem.* **2003**, *42*, 4382. [f] NHase enzyme from *Rhodococcus sp.* R312 in the presence of butyric acid. [g] Artaud, I.; Chatel, S.; Chauvin, A. S.; Bonnet, D.; Kopf, M. A.; Leduc, P. *Coord. Chem. Rev.* **1999**, *192*, 577−586. [@]Determined in CH_2Cl_2 solvent. NR = not reported.

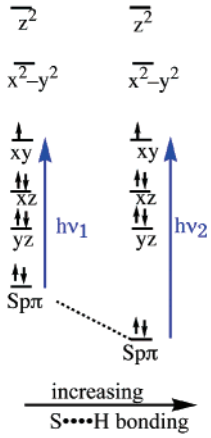

Figure 14. Partial MO diagram depicting the stabilization of πS orbitals and the resultant blue shift that would occur in the electronic spectrum due to H-bonding.

would stabilize any molecular orbital possessing sulfur character, including both the antibonding SOMO d_{xy}(Fe−S(π*)) and the bonding Sπ(Fe−S(π)) orbitals. Since both of these orbitals are involved in the charge-transfer transition observed near 700 nm, one would expect the energy of this transition to be affected only if the net H-bonding-induced stabilization is not identical for both orbitals. Since it protrudes more toward the solvent, one would expect the lower energy Sπ(Fe−S(π)) orbital with greater sulfur character to be stabilized more (Figure 14). The observed blue-shift (Figure 13) supports this description. The electronic spectrum of NHase is also sensitive to changes in H-bonding. However, with NHase the CT band red-shifts,[23] as opposed to blue-shifts, when the number of H-bonding donors is increased. This suggests that something other than H-bonding to the sulfurs, such as H-bonding to either the amide or sulfinate and/or sulfenates oxygens, is responsible for this shift with NHase.

2.7.1.1. Redox Inactivity. The majority of hydrolytic enzymes[95,96] utilize Zn^{2+}—a metal ion which is redox inactive in *all* ligand environments. Redox-active metals, such as iron, are usually avoided, because the reduced Fe^{2+} ion could be potentially damaging to the protein by promoting side reactions involving OH•. However, Zn^{2+}-containing enzymes usually hydrolyze substrates more electrophilic than RCN,[95,96] requiring less activation. The five anionic ligands (two deprotonated peptide amides and three cysteinates) coordinated to the Fe^{3+} ion of NHase create an environment that is highly stabilizing to iron in its 3+ oxidation state, and this would be expected to shut down redox activity. This is supported by synthetic modeling studies reported by Mascharak and co-workers,[54] which showed that when two amides and two aromatic thiolates are incorporated into the coordination sphere, the redox potentials of NHase analogues shift, anodically, to extremely low potentials. For example, carboxamide-ligated $[Fe^{III}(PyPepS)_2]^-$ (**7**; Figure 11) is reduced at a potential of −1.12 V, whereas imine-ligated $[Fe(III)(PyAS)_2]^+$ (**10**) is reduced at $E_{1/2}$ = −0.13 V vs SCE (Table 4).[54] This difference can be attributed, in part, to differences in molecular charge, since **7** is anionic, whereas **10** (Figure 11) is cationic. One would expect it to be more difficult to add an electron to an anionic complex. The alkanethiolate sulfurs (i.e., cysteinate sulfurs) of NHase also play an important role in shutting down redox activity, as is shown by the redox potentials (Table 4) of model complexes **4**−**6** (Figure 9).[64] These complexes incorporate two alkanethiolate ligands but lack anionic carboxamides, incorporating neutral imines in their place. Even though complexes **4**−**6** are cationic, their redox potentials are still fairly anodic and fall in the range $E_{1/2}$ = −0.72 to −1.02 V (vs SCE).[64] Replacement of the imine nitrogens in alkanethiolate-ligated **4**−**6** with carboxamides would be expected to shift these potentials to even more negative values (by ∼1 V based on Mascharak's observations),[54] since the overall molecular charge would become negative. Likewise, replacement of the aromatic thiolates in **7** (Figure 11) with alkanethiolates would be expected to shift Mascharak's potentials[54] to even more negative potentials. Together, these results indicate that *when iron is an environment resembling that of NHase, both the anionic amides and the alkanethiolate ligands contribute to making the Fe(II) oxida-*

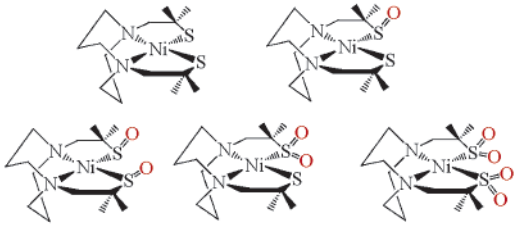

Figure 15. Darensbourg's Ni(II)−sulfenate and −sulfinate complexes derived from the DACO ligand.

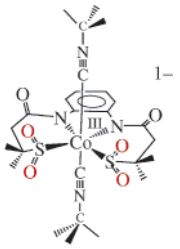

Figure 16. Artaud's six-coordinate sulfinate-ligated Co-NHase model complex $[Co^{III}(N_2(SO_2)_2)(CN^tBu)_2]^-$ (**11**).

tion state fairly inaccessible under biologically relevant conditions. This is important in order to avoid unwanted Fenton ($OH^•$) or H-atom abstraction chemistry.

2.7.2. Models Containing Oxygenated Sulfurs

The most comprehensive examination of metal−thiolate sulfur oxidation chemistry has been provided by Darensbourg and co-workers.[171−176] Darensbourg's group has shown for the series of Ni−thiolate complexes shown in Figure 15 that thiolate sulfur oxygenation increases the σ-donor properties of the sulfur and raises the redox potential, making the complexes easier to reduce. The M−S bond lengths either slightly decrease or increase, depending on the number of oxygen atoms added. Addition of a single oxygen atom increases the Ni−S bond lengths (from 2.15 to 2.16 Å), whereas addition of two oxygen atoms tends to decrease these bonds (from 2.15 to 2.12 Å).[171] The resulting S=O bonds are weaker in the singly oxygenated Ni−(RS=O) versus the doubly oxygenated Ni−(RS=$(O)_2$) complexes, as indicated by their longer S−O bonds (1.55 Å in Ni−(RS=O) vs 1.46 Å in Ni−(RS=$(O)_2$), lower $\nu_{S=O}$ stretching frequency (909−925 cm^{-1} in Ni−(RS=O) vs 1032−1192 cm^{-1} in Ni−(RS=$O)_2$),[171] and increased reactivity with oxygen-atom-abstracting agents.[176]

One would anticipate similar behavior with NHase. Oxygenation of the sulfur ligands would be expected to remove electron density from the metal ion, thereby increasing its Lewis acidity. Sulfur oxygenation would also "tie up" the sulfur's π-symmetry orbitals and "push" the ligand-centered orbitals further below the metal-centered orbitals (in energy). Solomon and co-workers have shown that the low-energy ligand-to-metal charge-transfer (LMCT) band characteristic of NHase involves the promotion of a π-symmetry sulfur electron into the half-occupied metal d_{xy} orbital.[167] For this transition to occur at low energies, it is required that at least one of the thiolate sulfurs remain unoxygenated. In NHase, the apical cysteinate, trans to the hydroxide (and potential "substrate binding" site), is the only sulfur that is reproducibly observed to be unoxygenated (Figure 4). The oxygenated sulfurs lie in the equatorial plane, cis to the hydroxide, and accessible to the solvent channel. Thus, the apical sulfur is at least partly, if not predominantly, responsible for the enzyme's intense color. How the deprotonated amides contribute to this chromophore remains to be investigated.

Sulfur oxidation of metal−thiolate complexes usually proceeds directly to the doubly oxygenated sulfinate (RS=$(O)_2$), since the singly oxygenated sulfenate (RS=O) is more reactive than its thiolate precursor. Singly oxygenated sulfenates are unstable unless coordinated to a metal ion,[103] and even then they can be difficult to trap.[177] For these reasons, most of the available synthetic NHase models possess doubly[157,158,163,178,179] rather than singly[69,150,177] oxygenated sulfurs. Oxidation of Co−thiolate complexes is typically easier than that of Fe−thiolates, since metal oxide (M_xO_y) formation (i.e., "rust" in the case of iron) is less favored for cobalt. Coordinatively saturated complexes are typically easier to oxidize than coordinatively unsaturated complexes, since pathways involving oxygen attack at the metal are unavailable.

There are a number of examples of coordinatively saturated Fe- or Co-NHase models that will react with O_2, epoxides, or H_2O_2 to afford the corresponding sulfinate analogue. For example, epoxidation of six-coordinate $[Co^{III}(N_2S_2)(CN^tBu)_2]^-$ affords the corresponding sulfinate complex $[Co^{III}(N_2(SO_2)_2)(CN^tBu)_2]^-$ (**11**; Figure 16).[163] Reaction of six-coordinate $[M^{III}(PyPepS)_2]^-$ (M = Co (**12**), Fe (**7**)) with H_2O_2 affords the corresponding sulfinate complex $[M^{III}(PyPepSO_2)_2]^-$ (M = Co (**13**), Fe (**8**); Figure 11).[158,178] The average Co^{III}−S distance decreases from 2.222(1) Å in **12** to 2.166(1) Å in **13** upon sulfur oxidation,[178] reflecting the increased ligand field of the sulfinato (RS(=$O)_2$) group. There are fewer examples of coordinatively unsaturated five-coordinate iron or cobalt−thiolate complexes that display clean sulfur oxygenation chemistry. In cases where sulfur oxidation does occur, structural rearrangement from the sulfur- to oxygen-bound sulfinate occurs if there is an open coordination site. For example, five-coordinate $[Fe^{III}(PyPS)]^-$ (**14**) reacts with O_2 to afford initially the corresponding sulfur-bound sulfinato complex $[Fe^{III}(PyP\{SO_2\})]^-$ (**15**; Figure 17),[157] which readily isomerizes to the corresponding O-bound linkage isomer $[Fe^{III}(PyP\{SO_2\})]^-$ (**16**; Figure 17). The O-bound linkage isomer is apparently the thermodynamically preferred isomer.

When the open coordination site of **15** is occupied by, for example, CN^-, structural rearrangement to the oxygen-coordinated linkage isomer is not observed.[157] Chottard's oxygen-bound sulfinate complex $[Fe^{III}(L\text{-}O_2)]^{2-}$ (**17**; Figure 17) provides another example illustrating this point.[179] The unoxygenated tris-thiolate-ligated precursor to **17** could not be isolated.[179] Oxygenation of the apical as opposed to equatorial sulfurs in **17**, coupled with its conversion to an O-linkage isomer, results in the stabilization of the $S = {}^3/_2$ as opposed to the $S = {}^1/_2$ spin-state. There are only three examples of synthetic NHase analogues that incorporate singly oxygenated sulfenate

BATCH: cr80a25 USER: slr69 DIV: @xyv04/data1/CLS_pj/GRP_cr/JOB_i80/DIV_cr020619e DATE: January 2, 2004

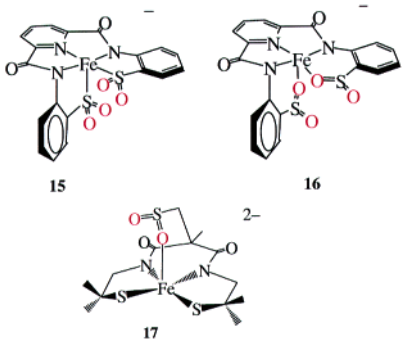

Figure 17. Five-coordinate sulfinato complex $[Fe^{III}(PyP\{SO_2\})]^-$ (**15**), which readily isomerizes from the sulfur-bound to the more stable oxygen-bound linkage isomer $[Fe^{III}(PyP\{SO_2\})]^-$ (**16**). Chottard preferentially isolates the oxygen-bound linkage isomer of five-coordinate sulfinate-ligated $[Fe^{III}(L\text{-}O_2)]^{2-}$ (**17**).

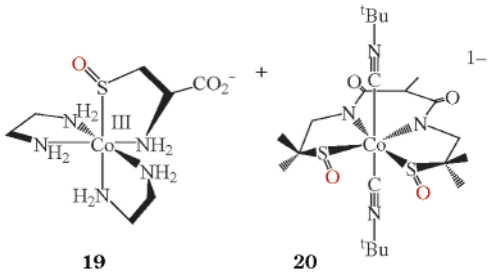

Figure 18. Rare examples of singly oxygenated cobalt sulfenate complexes $[Co^{III}(en)_2(SO\text{-}Cys)]^+$ (**19**) and $[Co^{III}(L\text{-}N_2SOSO)(^tBuNC)_2]^-$ (**20**).

(RS═O) sulfurs, and all of these contain cobalt.[69,150,177] Reaction of $[Co^{III}(en)_2(S\text{-}Cys)]^+$ (**18**) with singlet O_2 affords the corresponding sulfenate complex $[Co^{III}(en)_2(SO\text{-}Cys)]^+$ (**19**; Figure 18).[177] The mechanism for this reaction is proposed to involve initial attack by O_2 at the coordinated sulfur of **18** to afford a persulfoxide Co^{III}−(RS−O−O) intermediate, which then transfers an oxo atom to its thiolate precursor **18** to afford the final oxygenated product **19**.[177] Bis-sulfenate ligated $[Co^{III}(L\text{-}N_2SOSO)(^tBuNC)_2]^-$ (**20**; Figure 18) was synthesized via the addition of H_2O_2 to $[Co^{III}(L\text{-}N_2S_2)(^tBuNC)_2]^-$.[69] Despite being coordinatively saturated, **20** will hydrolyze nitriles via a mechanism proposed to involve the sulfenate ligand (vide infra). The third example, $[Co^{III}((\eta^2\text{-}SO)(SO_2)N_3(Pr,Pr))]^+$ (**21**; Figure 19), incorporates not only a singly oxygenated sulfur but a doubly oxygenated thiolate as well,[150] making it similar to the NHase active site.[101] The conformation of the sulfenate oxygen in **21**, syn with respect to the potential open binding site, is identical to its orientation in NHase. With **21**, both the sulfenate sulfur and oxygen coordinate in an η^2-binding mode.[150] This complex does not bind additional ligands, because the sulfenate oxygen binds to, and blocks access to, the open coordination site. This would suggest that the sulfenate oxygen of NHase $CysS^{114}$═O might interfere with activity by blocking the reactive site. The nearby conserved Arg residues (Arg^{56}, Arg^{141})[28,106] might prevent this by H-bonding to the sulfenate and thereby prevent an η^2-coordination mode. The η^2-binding mode also prevents further oxidation of the singly oxygenated sulfur. $[Co^{III}((\eta^2\text{-}SO)(SO_2)N_3(Pr,Pr))]^+$ (**21**; Figure 19) was synthesized via the stepwise oxidation of five-coordinate thiolate-ligated $[Co(III)(S_2{}^{Me_2}N_3(Pr,Pr))]^+$ (**23**; Figure 19). Only one of the thiolate sulfurs of **23** is oxidized upon addition of O_2 to afford $[Co(III)(S^{Me_2}(SO_2)N_3(Pr,Pr))]^+$ (**22**; Figure 19). In contrast to **23**, which readily binds azide and thiocyanate,[125,180] **22** does not bind additional ligands to its vacant coordination site. The remaining thiolate sulfur of **22** is oxidized (to afford **21**) only by H_2O_2, and a second oxygen is not added, even with prolonged reaction times and excess peroxide.[150]

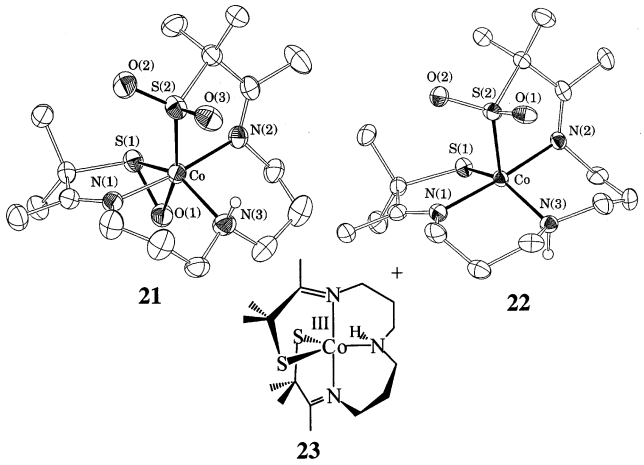

Figure 19. A NHase model complex $[Co^{III}((\eta^2\text{-}SO)(SO_2)N_3(Pr,Pr))]^+$ (**21**) that incorporates both a singly and a doubly oxygenated thiolate. The conformation of the sulfenate oxygen is syn with respect to the potential open binding site, making it identical in orientation to NHase. Sulfinate/sulfenate-ligated **21** is synthesized via H_2O_2 oxidation of doubly oxygenated **22**, which is obtained via O_2 oxidation of five-coordinate **23**.

2.8. Reactivity Models

In order for synthetic models and metalloenzyme sites to display reactivity, there must be an open or labile coordination site. With M^{III} (M = Fe, Co), six-coordinate, octahedral structures are highly favored and tend to be less reactive than, for example, five-coordinate structures, especially if the M^{III} ion is low-spin. Five-coordinate structures are difficult to isolate, however, in the absence of a protective protein pocket, or ligand constraints, especially when thiolates are included in the coordination sphere. Open coordination sites tend to encourage dimerization. Amide ligands tend to favor lower coordination numbers (i.e., <6) due to their high σ-donor capacity.[58] For example, the deprotonated amide ligand HMPA-DMP^{4-} affords a rare example[181] of a four-coordinate, square planar Co(III) complex, $[Co^{III}(\eta^4\text{-}HMPA\text{-}DMP)]^-$ (**24**; Figure 20). Addition of CH_3^+ to the carboxamide oxygens results in a more reactive neutral imine derivative, $[Co^{III}(\eta^4\text{-}(Me)HMPA\text{-}B)]$ (**25**; Figure 20),[58] containing a slightly more Lewis acidic Co^{III} ion. These common reactivity patterns associated with thiolate- and amide-ligated cobalt and iron suggest that the NHase protein and the amino acids located in the active site cavity (H-bonds, etc.), as well as the post-tranlationally modified sulfurs, play an important role in modifying the active site properties.

BATCH: cr80a25 USER: slr69 DIV: @xyv04/data1/CLS_pj/GRP_cr/JOB_i80/DIV_cr020619e DATE: January 2, 2004

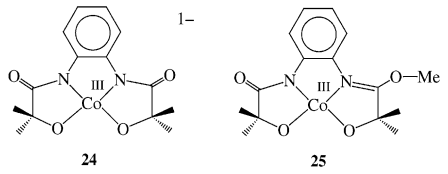

Figure 20. Low coordination number favored by amide ligated by anionic amide ligands $[Co^{III}(\eta^4\text{-HMPA-B})]^-$ (**24**) and its neutral iminoester derivative $[Co^{III}(\eta^4\text{-(Me)HMPA-B})]$ (**25**).

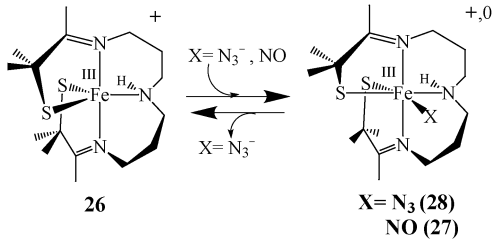

Figure 21. Reversible binding of azide and binding of NO to coordinatively unsaturated $[Fe^{III}(S_2{}^{Me_2}N_3(Pr,Pr))]^+$ (**26**).

2.8.1. Models That Bind Inhibitors

A five-coordinate synthetic analogue of the NHase intermediate observed upon low-temperature flash photolysis of NO from NO-inactivated NHase,[113] $[Fe^{III}(S_2{}^{Me_2}N_3(Pr,Pr))]^+$ (**26**; Figure 21), is obtained using a ligand that incorporates imine nitrogens.[65] The Mossbauer and EPR parameters associated with **26** compare well with those of this NHase intermediate.[182] Nitric oxide (NO) binds to **26**, trans to a thiolate sulfur, to afford a model for the NO-inactivated form of NHase $[Fe^{III}(S_2{}^{Me_2}N_3(Pr,Pr))(NO)]^+$ (**27**; Figure 22).[151,183] NO-bound **27** is diamagnetic and displays a highly perturbed electronic spectrum (λ_{max} = 420 nm) and NO stretching frequency ν_{NO} = 1822 cm^{-1} similar to that of NO-inactivated NHase (λ_{max} = 370 nm; ν_{NO} = 1853 cm^{-1}).[17,111] Coupling between the odd electron on NO and the odd electron on the metal, which resides in a π_{xy}*(Fe−S) orbital, is responsible for this large perturbation in electronic structure.[151] In the absence of light, *the Fe(III)−NO bond of* **27** *(Figure 22) is extremely robust, as indicated by the extremely short Fe−NO bond of 1.676(3) Å*. Photoexcitation of an electron into an σ*(Fe−NO) orbital results in the cleavage of the Fe−NO bond in **27**, as well as in NO-inactivated NHase.[17] This results in the reactivation of NHase. With **27**, however, photodecomposition of the iron product (**26**) of this photolysis makes the reaction irreversible. Grapperhaus showed that when NO binds trans to a nitrogen as opposed to a thiolate sulfur in $[(bmmp\text{-}TASN)Fe^{III}NO]^+$, the Fe^{III}−NO bond is even shorter (1.609(6) Å) than in **27**, and the ν_{NO} stretch (1856 cm^{-1}) more closely matches that of NHase (1852 cm^{-1}).[155]

Azide binds reversibly to **26**, trans to a thiolate sulfur (Figure 21), to afford a model for the azide-inhibited form of NHase $[Fe^{III}(S_2{}^{Me_2}N_3(Pr,Pr))(N_3)]$ (**28**; Figure 22).[65] Azide-bound **28** reproduces key magnetic and spectroscopic features of NHase, including its spin-state ($S = {}^1/_2$), low-energy electronic absorption (LMCT) band (λ_{max} = 708(1600) nm), and average metal−sulfur bond length (Table 3).[65] The EPR signals associated with azide-bound **28** (Table 2) are nearly identical to those of azide-inhibited NHase (Table 2).[52] The intense, low-energy sulfur-to-iron charge-transfer band seen with six-coordinate **28** is not seen with five-coordinate **26** (Table 1).[65] Most likely this is because the orbitals involved in the charge-transfer transition do not overlap as effectively when the S−M−S angles deviate significantly from 90°. A decrease in orbital overlap would be expected to decrease the intensity of the charge-transfer band.[5,139] With the exception of the NO-inhibited form, every form of Fe-NHase characterized to date displays an intense low-energy charge-transfer band. This *implies that Fe-NHase is either six-coordinate* or maintains a square pyramidal as opposed to trigonal bipyramidal geometry upon dissociation of ligands.

Consistent with Collins's observations regarding the tendency for carboxamide ligands to decrease the Lewis acidity of a metal ion,[58] Artaud found that carboxamido-ligated $[Co^{III}(N_2S_2)]^-$ (**29**; Figure 23) does not readily bind additional ligands—only strong π-acid ligands, such as cyanide (a NHase inhibitor),[184,185] and NO were found to bind to **29**.[162]

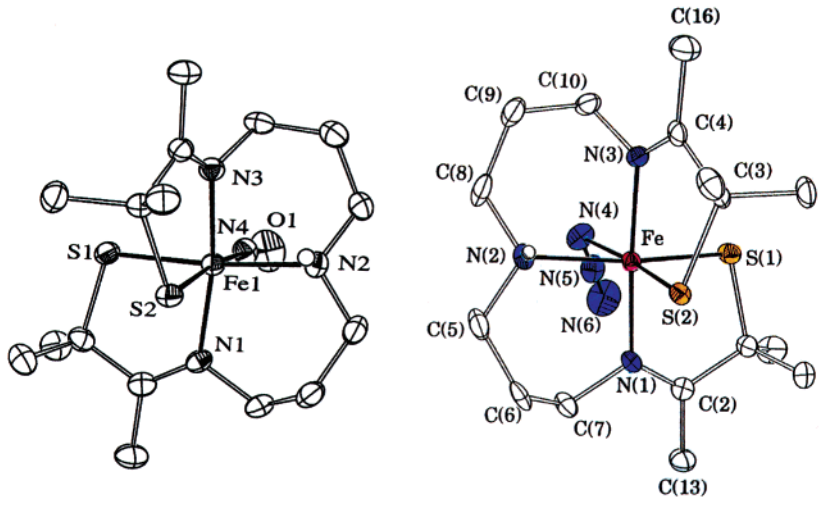

Figure 22. NO-inactivated and azide-inhibited NHase analogues $[Fe^{III}(S_2{}^{Me_2}N_3(Pr,Pr))(NO)]^+$ (**27**) and $[Fe^{III}(S_2{}^{Me_2}N_3(Pr,Pr))(N_3)]$ (**28**).

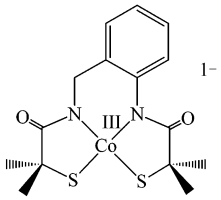

29

Figure 23. Artaud's carboxyamide-ligated $[Co^{III}(N_2S_2)]^-$ (**29**) does not readily bind additional (axial) ligands.

This curtailed reactivity suggests that *the equatorial ligand set of NHase significantly decreases the Lewis acidity of the metal center if the ligands coordinated to the metal center remain unmodified*. Incorporation of oxygens on the equatorial sulfurs,[99,124] and/or H-bonding to the carboxamides,[106] would increase the metal ion Lewis acidity and thus its tendency to bind additional ligands.

2.8.2. Hydroxide Binding

The resting state of NHase has been shown to contain a hydroxide coordinated to the Fe^{III} ion.[47,186] Two of the proposed mechanisms for nitrile hydrolysis by NHase involve this hydroxide as the active catalyst. Iron(III) hydroxides are in general unstable with respect to μ-oxo dimer formation,[146,187−190] and therefore they are difficult to isolate outside of a protein environment. Hydroxides are easily generated by Fe^{III}, because coordination of a water molecule by Fe^{III} causes the pK_a to drop significantly, to the point where it in many cases spontaneously deprotonates, even under mildy acidic conditions.[146,187,188,190,191] This is especially true with tricationic metal complexes. The large number of negatively charged residues bound to the Fe^{III} ion of NHase is likely to raise this pK_a. The S═O's[99] and H-bonded Arg's[106] would offset this somewhat.

The first structurally characterized example of a mononuclear Fe^{III}−OH complex, $[Fe^{III}(tnpa)(OH)(PhCOO)]^+$ (**30**; Figure 24; tnpa = tris(6-neopentylamino-2-pyridylmethyl)amine), was reported by Masuda in 1998.[192] Nitrogen-ligated **30** incorporates bulky neopentyl substitutents and amide N−H's in order to add stability to the terminal Fe^{III}−OH. Reactivity with hydrolyzable substrates such as RCN has not yet been reported. Borovik was also able to stabilize a terminal Fe^{III}−OH (**31**), as well as an Fe^{III}−oxo species (derived from dioxygen), using a tripodal encapsulating TREN amide ligand.[193] Both $[Fe^{III}(H_3\mathbf{1}^{But})(OH)]^-$ (**31**; Figure 24; $H_3\mathbf{1}^{But}$ = ($Bu^tNHC(O)CH_2)_3N$ = tris((N-*tert*-butylcarbamoyl)methyl)-amine) and $[Fe^{III}(H_3\mathbf{1}^{But})(O)]^{2-}$ (**32**) were isolated and crystallographically characterized.[193] Again, μ-oxo dimer formation is avoided by incorporating H-bonding residues and steric bulk. Nocera isolated a terminal Fe^{III}−OH using a "hangman" pophyrin, $[Fe^{III}(HPX\text{-}CO_2H)(OH)]$ (**33**; Figure 24; HPX = hanging porphyrin xanthene), containing bulky mesityl groups flanking the porphyrin ring, which preclude bis-iron(III) μ-oxo dimer formation, and a rigid spacer containing a single hydrogen-bonding RCO_2^- group.[194]

NHase model complex $[Fe^{III}(PyPS)]^-$ (**34**)[157] binds water at low temperatures to afford $[Fe^{III}(PyPS)(H_2O)]^-$ (**35**; Figure 25). The pK_a of the bound water

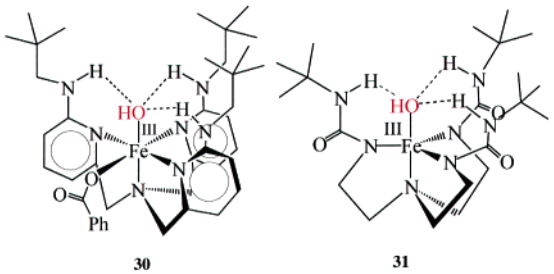

30 31

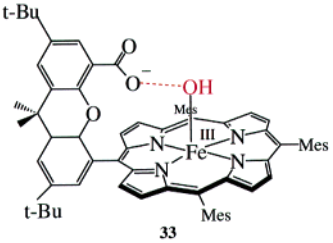

33

Figure 24. The first structurally characterized terminal Fe^{III}−OH $[Fe^{III}(tnpa)(OH)(PhCOO)]^+$ (**30**), Borovik's terminal Fe^{III}−OH complex $[Fe^{III}(H_3\mathbf{1}^{But})(OH)]^-$ (**31**; $H_3\mathbf{1}^{But}$ = $Bu^tNHC(O)(CH_2)_3N$ tris((N-*tert*-butylcarbamoyl)methyl)-amine), and Nocera's "hangman" porphyrin $[Fe^{III}(HPX\text{-}CO_2H)(OH)]$ (**33**; HPX = hanging porphyrin xanthene) containing a terminal Fe^{III}−OH.

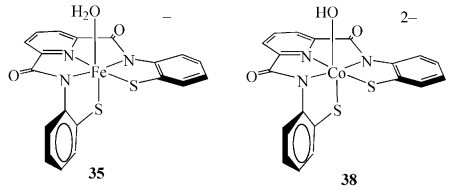

35 38

Figure 25. Mascharak's water- and hydroxide-ligated NHase model complexes $[Fe^{III}(PyPS)(H_2O)]^-$ (**35**) and $[Co^{III}(PyPS)(OH)]^{2-}$ (**38**). Complex **38** has been shown to slowly hydrolyze nitriles (18 turnovers in 4 h) at 50 °C and pH = 9.5.

molecule of **35** was found to be 6.3 ± 0.4, indicating that it would be readily deprotonated at physiological pH. The hydroxide derivative $[Fe^{III}(PyPS)(OH)]^{2-}$ (**36**) is generated in aqueous solution at pH = 10.0. Although μ-oxo dimer formation is usually difficult to avoid in the absence of built-in steric bulk,[146,187−190] there is no mention of μ-oxo dimer formation with carboxamido-ligated **36**. It is likely that the large accumulation of negative charge that would result (a μ-oxo dimer derivative of **36** would have an overall 4− charge) prevents μ-oxo formation in this case. Water-bound **35** and hydroxide-bound **36** have yet to be fully characterized. The cobalt analogue $[Co^{III}(PyPS)(H_2O)]^-$ (**37**) has also been generated in solution and has a slightly more basic coordinated water molecule pK_a = 8.30(3).[159] Oxygenation of one of the sulfurs in **37** shifts this pK_a to 7.20(6).[124] Water-ligated **37** can be converted to a hydroxide-bound derivative, $[Co^{III}(PyPS)(OH)]^{2-}$ (**38**; Figure 25), under basic conditions.[159] This Co(III) complex slowly hydrolyzes nitriles (vide infra). Because the water molecule of $[Fe^{III}(PyPS)(H_2O)]^-$ (**35**) is not displaced by nitriles,[157] it was concluded that nitriles do *not* bind to the NHase Fe site, and thus mechanisms 1 and 2 are more likely than mechanism 3. However, a slightly different model complex, $[Fe^{III}(S_2{}^{Me_2}N_3(Et,Pr)]^+$ (**39**; Figure 26),[126,195] was shown to bind nitriles

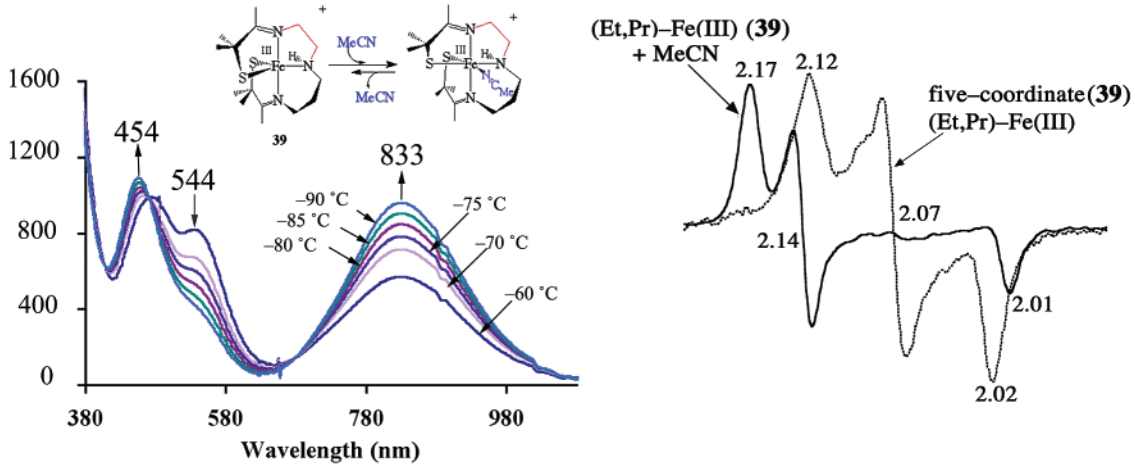

Figure 26. Variable-temperature UV/vis (−90 °C in CH_2Cl_2) and X-band EPR (CH_2Cl_2/toluene (1:1) glass, 150 K) spectrum showing that MeCN reversibly binds to $[Fe(III)(S_2^{Me_2}N_3(Et,Pr))]^+$ (**39**) at low temperatures.

Table 5. Rates of Ligand Exchange from Low-Spin Nitrile Hydratase Model Compounds

	k_{off} (s^{-1})	k_{on} (M^{-1} s^{-1})	$\Delta H^{\ddagger}$ (kcal mol^{-1})
$[Fe(III)(S_2^{Me_2}N_3(Et,Pr)(MeCN)]^+$ (**40**)[a]	$8.50(2) \times 10^4$		7.1 ± 0.8
$[Fe(III)(S_2^{Me_2}N_3$ (Et,Pr))(PhCN)$]^+$ [a]	$3.27(2) \times 10^4$		4.9 ± 0.8
$[Fe(III)(S_2^{Me_2}N_3(Et,Pr))(^i PrCN]^+$ [a]	$3.27(2) \times 10^4$		5.4 ± 0.6
$[Fe(III)(S^{Me_2}N_4(tren))(MeCN)]^{2+}$ [a]	$1.25(1) \times 10^1$		
$[Co(III)(S_2^{Me_2}N_3(Pr,Pr))(N_3)]$ (**23**-N_3)[b]	$2.1(5) \times 10^{-2}$	1.6 ± 9.5	
$[Co(III)(S_2^{Me_2}N_3(Pr,Pr))(SCN)]$ (**23**-SCN)[b]	$7.22(4) \times 10^{-1}$	$(3.6 \pm 0.6) \times 10^1$	
$[Co(III)(NH_3)_5(H_2O)]^{3+}$	5.7×10^{-6} [c]		
$[Fe(III)(S_2^{Me_2}N_3(Pr,Pr))(N_3)]$ (**28**)[b]	$1.4(5) \times 10^{-1}$	2.5 ± 0.3	

[a] Shearer, J.; Jackson, H. L.; Schweitzer, D.; Rittenberg, D. K.; Leavy, T. M.; Kaminsky, W.; Scarrow, R. C.; Kovacs, J. A. *J. Am. Chem. Soc.* **2002**, *124*, 11417. [b] Shearer, J.; Kung, I. Y.; Lovell, S.; Kaminsky, W.; Kovacs, J. A. *J. Am. Chem. Soc.* **2001**, *123*, 463. [c] Gonzalez, G.; Moullet, B.; Martinez, M.; Merbach, A. E. *Inorg. Chem.* **1994**, *33*, 2330.

(vide infra) with a K_{eq} that is an order of magnitude larger than that of MeOH (a ligand with a ligand field similar to that of water).

2.8.3. Models That Bind Nitriles

The only thiolate-ligated NHase model complex reported to bind nitriles, $[Fe(III)(S_2^{Me_2}N_3(Et,Pr))]^+$ (**39**), contains two imines and two alkanethiolates in the coordination sphere.[126,195] Nitrile binding is demonstrated by the variable-temperature UV/vis (−90 °C in CH_2Cl_2) and EPR (CH_2Cl_2/toluene (1:1) glass, 150 K) spectra ($g = 2.17$, 2.14, and 2.01) of **39**, shown in Figure 26 for RCN (R = Me). The intense band that grows in at 833(1010) nm is characteristic of six-coordinate, *cis*-thiolate Fe(III) complexes, including NHase, and indicates that five-coordinate **39** converts to a six-coordinate structure (Table 1), $[Fe^{III}(S_2^{Me_2}N_3$-$(Et,Pr))(MeCN)]^+$ (**40**), in the presence of acetonitrile. Nitrile binding to **39** is also supported by XAS.[126] The decrease in intensity of a pre-edge feature in the XANES spectrum corresponding to a 1s → 3d transistion indicates that the five-coordinate structure converts to a six-coordinate structure when MeCN is added. The EXAFS-determined mean Fe−S distance increases from 2.12 Å in CH_2Cl_2 to 2.17 Å in MeCN, which is also consistent with an increase in coordination number.[126] A wide variety of nitriles bind to **39**, including isopropionitrile, benzonitrile, and acetonitrile.[126] Alcohols such as MeOH or EtOH also bind to **39**, as indicated by changes in the EPR (g = 2.18, 2.15, and 2.00), UV/vis, XANES, and EXAFS spectra.[126] Thermodynamic parameters for acetonitrile ($\Delta H = -6.2 \pm 0.2$ kcal/mol, $\Delta S = -29.4 \pm 0.8$ eu), benzonitrile (-4.2 ± 0.6 kcal/mol, $\Delta S = -18 \pm 3$ eu), and pyridine ($\Delta H = -8 \pm 1$ kcal/mol, $\Delta S = -41 \pm 6$ eu) binding to $[Fe^{III}(S_2^{Me_2}N_3(Et,Pr))]^+$ were determined using variable-temperature electronic absorption spectroscopy.[126] Competitive binding studies demonstrate that MeCN preferentially binds over ROH (by an order of magnitude). Rates of nitrile exchange from $[Fe^{III}(S_2^{Me_2}N_3(Et,Pr))(RCN)]^+$ (**40**) are faster than one would expect for a low-spin Fe^{III} complex (Table 5),[126] and the corresponding activation parameters (determined using variable-temperature ^{13}C NMR line broadening) reflect this.[126] This *demonstrates that when contained in a ligand environment resembling that of NHase, low-spin Fe(III) is more labile than expected*. Increased lability is attributed to the *trans*-thiolate.[196] Replacement of this *trans*-thiolate with a nitrogen decreases nitrile exchange rates by 3 orders of magnitude.[126] Given that NHase also possesses a cysteinate sulfur trans to the exchangeable binding site, this *suggests that nature utilizes the labilizing effect of a trans-thiolate*[196] *to improve product dissociation rates*, and thus increase enzyme turnover rates.

2.8.4. Models That Hydrolyze Nitriles

Metal ions have been shown to enhance nitrile hydrolysis rates by as much as 10^6−10^7.[117,127,128,197,198] Furthermore, rate enhancement has been shown to be greater for 3+ vs 2+ metal ions. For example, $[Co(NH_3)_5(MeCN)]^{3+}$ stoichiometrically converts to $[Co(NH_3)_5(NHC(O)Me)]^{2+}$ via the external attack of OH^-

BATCH: cr80a25 USER: slr69 DIV: @xyv04/data1/CLS_pj/GRP_cr/JOB_i80/DIV_cr020619e DATE: January 2, 2004

Table 6. Rates of Nitrile Hydrolysis in the Absence or Presence of M^{3+} or M^{2+} Ions, Mercaptoethanol, or NHase Enzyme

	nitrile hydrolysis rate
$[Co^{III}(NH_3)_5(MeCN)]^{3+}$ [a]	3.40 M^{-1} s^{-1} @
free MeCN[b]	1.60×10^{-6} M^{-1} s^{-1} @
free PhCN[b]	8.2×10^{-6} M^{-1} s^{-1} @
$[Co^{III}(cyclen)(H_2O)_2]^{3+}$ [c]	4.7×10^{-3} s^{-1} **
$[Ru^{III}(NH_3)_5(MeCN)]^{3+}$ [d]	220 s^{-1}
$[Ru^{II}(NH_3)_5(MeCN)]^{2+}$ [d]	$<6 \times 10^{-5}$ s^{-1}
$[Co^{III}(PyPS)(OH)]^{2-}$ [e]	1.25×10^{-3} M^{-1} s^{-1}
$[Co^{III}(L\text{-}N_2SOSO)(^tBuNC)_2]^-$ [f]	5.79×10^{-4} M^{-1} s^{-1}
$HOCH_2CH_2SH$[g]	1.6×10^{-3} M^{-1} s^{-1} @
NHase (*Rhodococcus sp.* N-771)[h]	1600 μmol-product·min^{-1}·mg-protein$^-$ &

[a] Buckingham, D. A.; Keene, F. R.; Sargeson, A. M. *J. Am. Chem. Soc.* **1973**, *95*, 5649. [b] Rabinovitch, B. S. W., C. A. *Can. J. Res.* **1949**, *20B*, 185. [c] Kim, J. H.; Britten, J.; Chin, J. *J. Am. Chem. Soc.* **1993**, *115*, 3618. [d] Zanella, A. W.; Ford, P. C. *Inorg. Chem.* **1975**, *14*, 42. [e] Noveron, J. C.; Olmstead, M. M.; Mascharak, P. K. *J. Am. Chem. Soc.* **1999**, *121*, 3553. [f] Heinrich, L. M. V., A.; Li, Y.; Vaissermann, J.; Chottard, J.-C. *Eur. J. Inorg. Chem.* **2001**, 2203. [g] Cordes, E. H.; Zervos, C. *J. Org. Chem.* **1971**, *36*, 1661. Komeda, H. H., UY.; Kobayashi, M.; Shimizu, *Proc. Natl. Acad. Sci. U.S.A.* **1996**, *93*, 10572. [h] Piersma, S. R.; Nojiri, M.; Tsujimura, M.; Noguchi, T.; Odaka, M.; Yohda, M.; Inoue, Y.; Endo, I. *J. Inorg. Biochem.* **2000**, *80*, 283−288. @Per mole of OH^- under basic conditions. **Rate for intramolecular attack of a coordinated MeCN by *cis*-hydroxide (product release (3.3×10^{-4} s^{-1}) is rate-limiting. &V_{max}.

at the coordinated nitrile carbon at a rate of 3.40 M^{-1} s^{-1} at 25 °C (Table 6).[197] In contrast, the rate constant for hydrolysis of a free RCN, k_{OH}, is equal to 1.60×10^{-6} and 8.2×10^{-6} M^{-1} s^{-1}, for R = Me and Ph, respectively, under basic conditions at 25 °C. Coordinated aromatic nitriles, 3- and 4-formylbenzonitrile, are hydrolyzed by this Co(III) complex at rates of 117 and 142 M^{-1} s^{-1} respectively, with activation parameters of $\Delta H^{\ddagger} = 15.4$ kcal/mol, $\Delta S^{\ddagger} = +2$ eu, and $\Delta H^{\ddagger} = 16.0$ kcal/mol, $\Delta S^{\ddagger} = +5$ eu, respectively.[198] Chin showed that $[Co(cyclen)(OH_2)_2]^{3+}$ (cyclen = 1,4,7,10-tetraazacyclododecane) will catalyze the hydration of MeCN to acetamide at pH = 7 and 40 °C via the intramolecular attack of a hydroxide coordinated cis to a coordinated nitrile, with a rate constant of $k = 4.7 \times 10^{-3}$ s^{-1} (Table 6).[128] Both the MeCN-coordinated and acetamide-coordinated intermediates are detected in this reaction. Product (amide) release is the rate-limiting step of this reaction, with $k = 3.3 \times 10^{-4}$ s^{-1}.[128] Ford and co-workers have shown that by coordinating nitriles to a metal ion, nitrile hydrolysis rates are enhanced by as much as 10^6 relative to those in the absence of the metal ion.[127] Metal ions in the 3+ oxidation state were shown to enhance rates more than those in the 2+ oxidation state (Table 6).[127] This is illustrated by the hydrolysis chemistry of $[Ru^{II}(NH_3)_5(MeCN)]^{2+}$, which does not become a viable catalyst until the metal ion is oxidized to the 3+ oxidation state (Table 6).[117,127] This suggests that the metal ion in these catalysts activates the nitrile by acting as a Lewis acid (i.e., via an inductive effect), as opposed to via π-back-donation into the nitrile π^* orbitals. Given that Lewis acidity depends on the charge-to-size ratio (z/r), *it is likely that if nitriles coordinate to the NHase M^{3+} ion, both the higher oxidation state and the low spin-state of NHase play important roles in promoting nitrile hydrolysis.* The low spin-state would contribute to increasing Lewis acidity by decreasing the metal ion size.

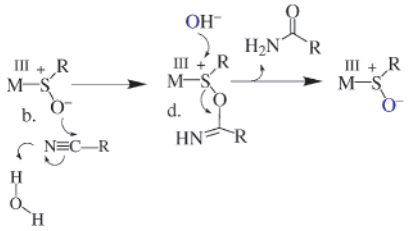

Figure 27. Proposed mechanism of nitrile hydrolysis by a metal-bound sulfenate ligand.

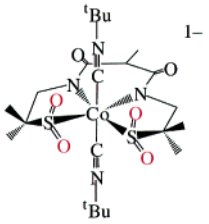

Figure 28. In contrast to singly oxygenated **20**, doubly oxygenated $[Co^{III}(L\text{-}N_2SO_2SO_2)(t\text{BuNC})_2]^-$ (**41**) does not hydrolyze nitriles.

The first thiolate-ligated NHase model complex to catalyze nitrile hydrolysis was reported by Mascharak in early 1999.[159] Under basic conditions, the hydroxide-ligated cobalt complex $[Co^{III}(PyPS)(OH)]^{2-}$ (**38**; Figure 25) slowly hydrolyzes nitriles (18 turnovers in 4 h; Table 6) at 50 °C and pH = 9.5, presumably via mechanism 1 or 2 of Figure 6. A more detailed mechanistic study has yet to be reported. In 2001, Chottard and co-workers reported that sulfenate-ligated $[Co^{III}(L\text{-}N_2SOSO)(t\text{BuNC})_2]^-$ (**20**, Figure 18) will slowly hydrolyze nitriles (50 turnovers in 24 h) at 4 °C under acidic conditions (pH = 4.8; Table 6)).[69] It was proposed that a singly oxygenated sulfenate oxygen is intimately involved in the mechanism of this system (Figure 27), and that this may also be the case with NHase. A mechanism of this sort would not involve the coordination of substrate to the metal ion, and thus would avoid the need for product displacement from a low-spin (substitution-inert) metal ion. However, as demonstrated by the slow rates (with **20**), the mechanism shown in Figure 27 does not benefit from the lowered activation barrier made possible via coordination to a Lewis acidic metal ion. Evidence for a mechanism involving the sulfenate oxygen of **20** (Figure 18) is three-fold. First, the fact that the metal ion of **20** is coordinatively saturated, and does not contain exchangeable ligands (isonitriles are strong-field ligands, and multidentate ligands, especially amides, do not readily dissociate), rules out a reaction mechanism involving nitrile coordination to the metal ion. Second, the analogous sulfinate derivative $[Co^{III}(L\text{-}N_2SO_2SO_2)(t\text{BuNC})_2]^-$ (**41**; Figure 28) containing doubly oxygenated sulfurs does not hydrolyze nitriles, implying that the singly oxygenated sulfurs are needed.[69] This would be consistent with the more reactive nature of free sulfenates (RS=O) vs sulfinates ($RS(=O)_2$)[103] and the weaker S=O bond of metal-coordinated sulfenates vs sulfinates.[171,176] Third, ^{18}O-labels are incorporated into the sulfenate of **20**, but not the

BATCH: cr80a25 USER: slr69 DIV: @xyv04/data1/CLS_pj/GRP_cr/JOB_i80/DIV_cr020619e DATE: January 2, 2004

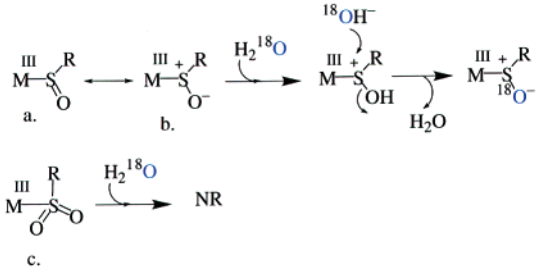

Figure 29. ^{18}O exchange reaction observed with singly oxygenated sulfenate but not doubly oxygenated sulfinate complexes.

sulfinate of **41**, via $H_2{}^{18}O$ exchange (Figure 29).[69] Although a more detailed mechanistic study involving Chottard's system[69] has yet to be been reported, the work is supported by similar results obtained by Deutsch and co-workers. Deutsch showed that the Co^{III}-coordinated sulfenate oxygens in $[(en)_2Co^{III}(S(O)CH_2CH_2NH_2)]^{2+}$ (**42**) behave as nucleophiles and will react with Lewis acids such as BF_3 and H^+.[70,71]

This suggests that when coordinated to a Co^{III} center, the sulfur oxygen bond of a sulfenate is significantly polarized, and resonance form "b" of Figure 29 dominates. The rather electron-rich environment of NHase would be expected to favor this resonance form even more, since it would place a positively charged sulfur next to the electron-rich metal ion. This is supported by recent DFT calculations which show that the sulfinate residue Cys^{112}-S═O in NHase is very strongly polarized.[112] The sulfur atom of Cys^{112}-S═O is predicted by these calculations to be the most positively charged center of the NHase active site.[112]

2.8.5. Making Low-Spin Co(III) More Reactive

If substrates coordinate to the metal ion of NHase as shown in mechanisms 2 and 3 of Figure 6, an obvious question with regard to Co-NHase concerns the usual lack of ligand exchange seen with Co(III) that would be expected to disfavor product dissociation. As stated by Lippard and Berg,[136] "Very inert first-row metals such as Co(III) are only rarely encountered in bioinorganic chemistry." Kovacs showed, however, that when anionic sulfur ligands are incorporated into the coordination sphere, ligand substitution rates for low-spin Co(III) can be dramatically increased.[125] This is also supported by Mascharak's observations that cyanide readily dissociates from low-spin $[Co^{III}(PyPS)(CN)]^{2-}$.[159] Five-coordinate $[Co^{III}(S_2{}^{Me_2}N_3(Pr,Pr))]^+$ (**23**; Figure 19), which contains Co(III) in an environment resembling that of NHase, was shown to reversibly bind N_3^-, SCN^-, and NH_3 (Figure 30).[180] Dissociation rate constants (Table 5) for **23**-N_3 and **23**-SCN are comparable to those of its Fe(III) analogue, **26**,[125] and are at least 4 orders of magnitude faster than that of $[Co(III)(NH_3)_5(H_2O)]^{3+}$ (Table 5).[199] These faster than usual exchange rates could be attributed either to the presence of a higher (S = 1 or 2) spin-state that is partially populated at the temperatures of these experiments,[200] or to the *trans*-thiolate sulfur ligand which is expected to have a labilizing effect.[196,201] Temperature-dependent magnetic studies show no

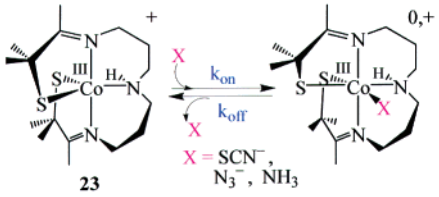

Figure 30. Ligand exchange from a low-spin (S = 0) d^6 Co^{III} ion is observed when ligands bind trans to a thiolate sulfur.

thermally accessible higher spin-states with **23**-N_3 or **23**-SCN, suggesting that the latter explanation is responsible. *This implies that the trans-thiolate sulfur plays an important role in promoting NHase reactivity*.

3. Superoxide Reductase (SOR)

3.1. Enzyme Function

Superoxide reductases (SORs) remove potentially toxic superoxide[29−42,202,203] from anaerobic organisms without forming O_2 as a side product.[33] The more well-known superoxide dismutases (SODs),[204] on the other hand, afford an equivalent of O_2 for every two molecules of $O_2^{\bullet-}$ destroyed. Oxidations mediated by superoxide are implicated in a number of important degenerative diseases. For example, the cell death and tissue damage that occurs following a stroke or heart attack is known to be caused by the high concentrations of O_2^- that build up following such an event.[205,206] Severe neurological disorders such as Parkinson's[207,208] and Alzheimer's[209−211] disease may also be related to nerve cell damage caused by O_2^-. Some types of cancer are thought to arise from oncogene mutations caused by O_2^--induced oxidative damage to DNA.[212,213]

3.2. Active Site Structure and Mechanism

Three crystal structures of SOR have been reported from two different bacterial sources—*Pyrococcus furiosus*[34] and *Desulfovibrio desulfuricans*.[214,215] In the catalytically active reduced state (Figure 31A), SOR contains a high-spin (S = 2) Fe^{II} center (center II) ligated by four equatorial histidines and one apical cysteinate trans to an open site. In the oxidized resting state (Figure 31B), the iron is high-spin (S = $^5/_2$) and contains a glutamate (Glu^{14} or Glu^{47} depend-

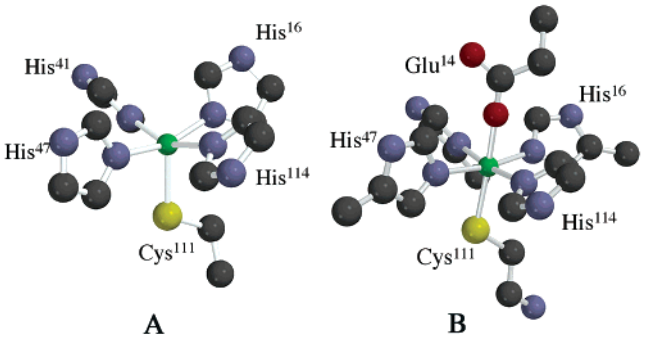

Figure 31. Structure of the reduced catalytically active Fe^{II} (A) and the oxidized glutamate-bound Fe^{III} (B) states of SOR.

BATCH: cr80a25 USER: slr69 DIV: @xyv04/data1/CLS_pj/GRP_cr/JOB_i80/DIV_cr020619e DATE: January 2, 2004

ing on the organism) coordinated to the sixth axial site. This glutamate (Glu^{14} and Glu^{47}) is attached to a solvent-exposed flexible loop region of the protein and moves to a distance of 7.1 Å away from the metal ion upon reduction to the Fe^{II} state.[34] This flexible loop region also contains a *conserved lysine* (Lys^{47} in desulfoferrodoxin;[214] Lys^{48} in *Desulfoarculus baarsii*) that has been shown to be essential for catalytic activity.[30] The ammonium group of Lys^{47} (or Lys^{48}) lies 6−12 Å away from the iron center. One of the key steps in the mechanism of superoxide reduction by SOR is proposed to involve the transfer of a proton from this Lys residue to metal-bound intermediates (vide infra).[38]

An obvious question regarding function concerns the ability of SORs to selectively reduce, as opposed to disproportionate, superoxide. The more extensively studied metalloenzyme, superoxide dismutase (SOD), disproportionates O_2^- to afford H_2O_2 and O_2.[204,216] The active site's redox potential and access to protons would be the two most important parameters governing this chemistry. The metal ion of SOR sits at the surface of the protein exposed to solvent.[34,214] The redox potential of the SOR Fe^{2+}/Fe^{3+} couple has been reported to fall in the range from 0.00 to −0.15 V vs SCE.[73,74,214,217−219] This redox potential range is high enough to make the reduced Fe^{II} form readily accessible (in fact, SOR has been shown to slowly autoreduce, even in air),[35] but at the same time is not too high, so that reduction of superoxide is still favored. The redox potential of superoxide (O_2^-) is highly dependent on pH. It is significantly easier to reduce under acidic conditions—at pH = 0, superoxide is reduced at a potential of +1.27 V vs SCE, whereas at pH = 7.5 and pH = 14, it is reduced at +0.83 and −0.041 V, respectively. If SOR-catalyzed superoxide reduction involves outer-sphere electron transfer, then *protons are probably used to raise the redox potential of superoxide and drive its reduction*. If superoxide reduction occurs via an inner-sphere electron mechanism, on the other hand, then redox potentials would be less important. Organisms containing SORs are anaerobic, and therefore not equipped to deal with the dioxygen product that would result from superoxide oxidation (one of the two half-reactions occurring with SODs). Superoxide oxidation is favored in the absence of a proton source, as indicated by the redox potential of the O_2^-/O_2 couple (−0.80 V vs SCE at pH = 14), which is significantly lower than when protons are present (−0.13 V vs SCE at pH = 0). Thus, the redox potential of the SOR Fe^{2+}/Fe^{3+} couple vs superoxide indicates that outer-sphere reduction of superoxide would be thermodynamically favored, as long as protons are available. Both inner-sphere and outer-sphere mechanisms require protons to cleave an Fe−O bond and/or to stabilize the peroxide product (H_2O_2). Thus, *protons play an important role in governing the chemistry that occurs at the SOR active site*. Placement of the active site close to the surface of the protein,[34] with the open binding site accessible to solvent, provides a constant pool of protons and access to the metal site. By burying the active site with SODs, on the other hand, proton delivery is perhaps more controlled, and protons are less accessible, making it possible to drive superoxide oxidation.

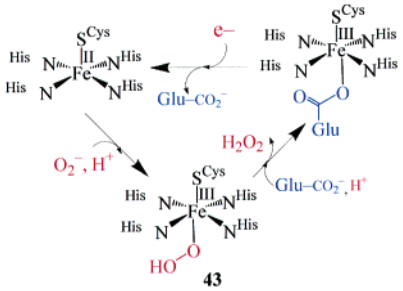

Figure 32. Proposed catalytic mechanism of superoxide reduction by superoxide reductases (SORs) involving an end-on hydroperoxide intermediate **43**.

The mechanism by which SORs are proposed to reduce superoxide is shown in Figure 32. Superoxide is proposed to bind to the reduced Fe^{II} state of SOR at diffusion controlled rates ($>10^9$ M^{-1} s^{-1}). The transfer of an electron from the metal ion to the bound substrate via an inner-sphere pathway is then proposed to afford an Fe^{III}−peroxide intermediate (**43**).[29−31,38,39] This intermediate is observed in pulse radiolysis experiments by electronic absorption spectroscopy.[30,31] Consistent with an inner-sphere pathway, exogenous ligands such as azide, nitric oxide, and cyanide have been shown to bind to the iron site of SOR.[36] Upon release of hydrogen peroxide, a nearby glutamate (Glu^{14} in *Pyrococcus furiosus*[34] and Glu^{47} in *Desulfovibrio vulgaris*)[30] coordinates to the iron center to afford the six-coordinate, Fe^{III}-oxidized resting state (Figure 31B). The proposed peroxide intermediate (**43**; Figure 32) displays a charge-transfer band at 600(∼3500)nm[35] and releases H_2O_2 at a rate of 40−50 s^{-1}.[31,38,73] The intense low-energy charge-transfer band associated with this intermediate was originally assigned as a combination peroxide/sulfur-to-metal charge-transfer transition,[31] but more recently it was suggested that this band is too low in energy for peroxide to be involved.[36] Recent DFT calculations suggest that this transition is mainly ^{Cys}S-to-Fe(III) charge transfer in character.[38]

When Glu^{47} is replaced with an alanine (in an E47A SOR mutant of *Desulfoarculus baarsii*), a transient intermediate is observed by resonance Raman that displays ν_{O-O} and ν_{Fe-O} stretches at 850 and 438 cm^{-1}, respectively.[29] These stretches shift to 802 and 415 cm^{-1} in the ^{18}O-labeled spectrum.[29] Stretching frequencies in this range are consistent with a metal−peroxide species. Mononuclear Fe^{III}−peroxide species have also been proposed, or identified, in the catalytic cycles of the antitumor drug bleomycin,[220] heme oxygenase,[221] cytochrome P450,[66,67] and Rieske dioxygenases.[4,7,222] With synthetic systems, peroxides have been shown to bind to iron in either an end-on or a side-on fashion (Figure 33).[152,223,224] Side-on iron−peroxides tend to have weaker Fe−O and stronger O−O bonds relative to end-on peroxides. This is reflected in the ν_{Fe-O} and ν_{O-O} stretching frequencies, which fall in the range 438−503 and 816−850 cm^{-1}, respectively, for a side-on peroxide, versus 609−644 and 781−806 cm^{-1}, respectively, for an end-on peroxide.[152,223,224] Side-on

BATCH: cr80a25 USER: slr69 DIV: @xyv04/data1/CLS_pj/GRP_cr/JOB_i80/DIV_cr020619e DATE: January 2, 2004

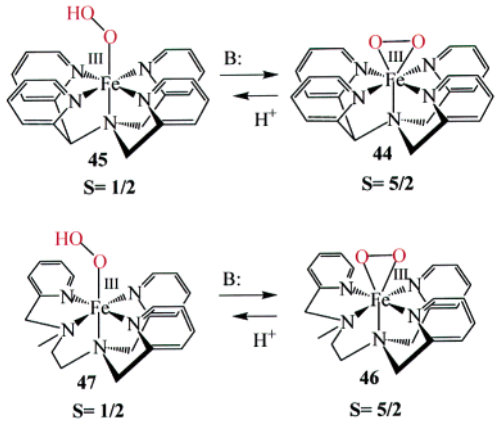

Figure 33. Synthetic end-on and side-on peroxide complexes $[(N_4Py)Fe^{III}(\eta^2\text{-}O_2)]^+$ (**44**), $[(N_4Py)Fe^{III}(\eta^1\text{-}OOH)]^{2+}$ (**45**), $[(trispicMeen)Fe^{III}(\eta^2\text{-}O_2)]^+$ (**46**), and $[(trispicMeen)\text{-}Fe^{III}(\eta^1\text{-}OOH)]^{2+}$ (**47**).

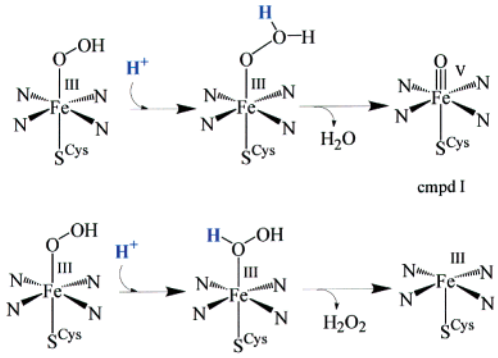

Figure 34. Summary of Harris and Loew's theoretical study, which shows that the site of protonation plays an important role in determining whether the O—O or Fe—O bond of cytochrome P450 cleaves.

Fe—peroxides tend to be high-spin ($S = {}^5/_2$), and end-on Fe—peroxides tend to be low-spin ($S = {}^1/_2$), at least based on the only available examples (Figure 33).[152,223,224] On the basis of its spin-state ($S = {}^5/_2$; $g = 4.3$) and ν_{O-O} and ν_{Fe-O} vibrational frequencies and comparison with known synthetic peroxides,[152,223,224] the E47A SOR mutant intermediate was described as a side-on ferric peroxide species.[29] The double-labeling ($^{18}O-^{16}O^-$) experiment required to varify this proposal has yet to be reported. Currently, the only structurally characterized biological example of a side-on-coordinated O_2 species[225] is naphthalene dioxygenase, a non-heme iron enzyme.[7] With SOR, it is not clear whether a similar side-on peroxide would form in the native enzyme, or whether the Glu → Ala mutation is responsible for its formation, if indeed it forms in this mutant. Recent DFT calculations comparing the stability of possible SOR intermediates suggest that a side-on peroxide would be much less stable than an end-on peroxide.[38]

As mentioned earlier, the active site of reduced SOR resembles that of the heme iron site of cytochrome P450 (Figure 2). The P450 analogy goes even further in that both SOR and cytochrome P450 have been proposed to form end-on hydroperoxide (Fe^{III}—OOH; Figures 32 and 34) intermediates during their catalytic cycle.[51,67] The major difference is that the O—O bond is cleaved with P450, whereas the Fe—O bond is cleaved with SOR. With SOR, it has been suggested that the trans cysteinate sulfur assists in promoting reduction of superoxide by "pushing" electron density onto the metal ion, and promotes cleavage of the Fe—O bond via its trans effect.[36] With P450, on the other hand, the trans cysteinate sulfur is proposed to play a critical role in promoting O—O bond cleavage and creating a reactive oxidation catalyst via the back-donation of electron density from the sulfur to orbitals possessing antibonding O—O character.[51,66–68] Differences in spin-state may be, in part, responsible for these differences in reactivity.[37,226] An $S = {}^5/_2$ peroxide would have populated antibonding σ^*(Fe—O) orbitals, thus favoring Fe—O bond cleavage. The peroxide intermediate of the E47A SOR mutant is $S = {}^5/_2$.[29] However, the same may not be true of the native enzyme. Recent calculations suggest that the peroxide-bound SOR intermediate is $S = {}^1/_2$.[38] However, there is no experimental evidence to confirm this. The low spin-state of the hydroperoxide P450 intermediate stabilizes the Fe—O bond and, as shown by Harris and Loew[51] as well as Solomon and co-workers for related non-heme iron systems,[227] weakens the O—O bond.[226] The site of protonation has also been shown to play a significant role in determining whether Fe—O or O—O bond cleavage occurrs (Figure 34).[51] Both the Fe—O and O—O bond cleavage steps of SOR and P450, respectively, are believed to be proton-assisted. With P450, protonation of the distal oxygen polarizes the O—O bond, making heterolytic cleavage favorable (Figure 34).[51] With SOR, protonation of the proximal oxygen would weaken the Fe—O bond, making Fe—O bond cleavage favorable (Figure 32).[38] There is no evidence for oxygenase activity with SOR, suggesting that the O—O bond cleavage does not occur, and reduced Fe^{II}—SOR is believed to be unreactive toward O_2.[35,38]

3.3. Exogenous Ligand Binding

Johnson and co-workers have spectroscopically probed the SOR superoxide binding site via the addition of exogenous ligands such as N_3^-, CN^-, and NO.[36,37] SOR is inhibited by cyanide[228] but not by azide. Spectroscopic studies indicate that both azide and cyanide bind to the SOR iron site, in both its reduced and oxidized states.[36] A possible mechanism for cyanide inhibition of SOR activity would involve cyanide coordinating to the open coordination site of the catalytically active Fe^{2+} site. This would make the Fe site inaccessible to O_2^-. However, this would not explain why SOR is not inhibited by azide. Another possibility is that CN^- inhibition involves the oxidized state. Given that the electronic properties of the oxidized SOR iron site are dramatically altered by cyanide but not by azide,[36] this represents a likely possibility. Oxidized SOR is characterized by an intense low-energy sulfur-to-iron charge-transfer band[217] at 660(2500) nm[36] that is sensitive to changes in pH and mutations of residues near the active site, as well as the addition of exogenous ligands. Mutation of the Glu[47] residue (from *Desulfoarculus baarsii*) to an Ala causes the LMCT band of wild-type oxidized SOR to blue-shift from 660 to 580(1800) nm.[30] It has been suggested that this is caused by the replacement

BATCH: cr80a25 USER: slr69 DIV: @xyv04/data1/CLS_pj/GRP_cr/JOB_i80/DIV_cr020619e DATE: January 2, 2004

of the coordinated carboxylate with a water. A shift in pH from 7.5 to 10.0 in wild-type SOR (obtained from *Pyrococcus furiosus*) causes the LMCT band to blue-shift from 660 to 590 nm.[36] Cyanide causes this band to red-shift to 685(2700) nm, whereas azide does not induce a noticeable shift.[36] Cyanide also induces a spin-state change from $S = {}^5/_2$ (in the oxidized Glu-bound resting state) to $S = {}^1/_2$ ($g = 2.29$, 2.25, and 1.94 in *Pyrococcus furiosus*; $g_{perp} = 2.27$,[36] $g_{||} = 1.96$ in *Desulfovibrio desulfuricans*).[229] Azide, on the other hand, does not cause the spin-state to change.[36] It is assumed that both N_3^- and CN^- displace the glutamate when they bind to the oxidized SOR active site.

With its odd electron, nitric oxide (NO) is used in many cases to probe spectroscopically silent metal ions in biology, such as Fe^{2+},[5,140] in order to get detailed information about the metal ion's electronic structure.[230] The frontier orbitals, and thermal stability of complexes derived therefrom, make NO a convenient mimic of dioxygen and its activated derivatives. When nitric oxide interacts with the Fe^{II} ion of SOR in its catalytically active state, an electron is transferred from the metal ion to the NO via an inner-sphere mechanism to afford a species which is best described electronically as an $Fe^{III}-NO^-$ species.[37] This is analogous to the mechanism by which superoxide is proposed to undergo reduction. The electronic absorption spectrum of this NO-bound SOR derivative is dominated by a fairly intense $\pi^*(NO^-)$-to-Fe^{3+} charge-transfer band at 475(530) nm.[37] The NO-bound SOR Fe^{III} ion is high-spin ($S = {}^5/_2$), as is the only $Fe^{III}-O_2^{2-}$ SOR derivative characterized so far.[29] With Fe−NO SOR, the two odd electrons on the NO^- couple antiferromagnetically to two of the five unpaired electrons on the Fe^{III}, resulting in an overall spin of ${}^3/_2$, as shown by the EPR parameters ($g = 4.34$, 3.76, and 2.00).[37] A similar $S = {}^3/_2$ EPR signal is observed when NO binds to other non-heme Fe^{II} enzymes.[230] The vibrational spectrum of Fe−NO SOR contains a ν_{N-O} stretch at 1721 cm^{-1} and a ν_{Fe-NO} stretch at 475 cm^{-1}, consistent with a reduced NO (NO^-) and a fairly weak Fe−NO bond. The population of σ^* antibonding orbitals in a high-spin $Fe^{III}-NO^-$ would be expected to contribute to the weakening of this Fe−NO bond. By analogy, it is argued that the similar electronic structure of the SOR Fe^{III}−peroxo intermediate would favor cleavage of the Fe−O bond, as opposed to the O−O bond, favoring peroxide release as opposed to cytochrome P450-type oxidation chemistry (Figure 34).[37] In contrast to NHase, the NO of NO−SOR is not photolabile.

3.4. Biomimetic Models of SOR

The spectroscopic characterization and isolation of Fe^{III}−peroxo complexes is extremely difficult owing to their high reactivity and photolability.[5,227,231,232] Only recently have biomimetic analogues of reactive metal−oxygen species been generated and characterized at low temperatures.[152,223,224,226,233−238] Que and Girerd have reported the most extensively characterized set of synthetic side-on ($Fe^{III}(\eta^2\text{-}O_2)$) or end-on ($Fe^{III}(\eta^1\text{-}OOH)$) non-heme iron peroxides.[82,223] These include $[(N_4Py)Fe^{III}(\eta^2\text{-}O_2)]^+$ (**44**; Figure 33),[225,240] $[(trispicMeen)Fe^{III}(\eta^2\text{-}O_2)]^+$ (**46**, Figure 33),[226,236−238]

Figure 35. Halfen's reduced SOR model complex $[(L^8py_2)\text{-}Fe^{II}(SAr)]^+$ (**48**).

$[(N_4Py)Fe^{III}(\eta^1\text{-}OOH)]^{2+}$ (**45**; Figure 33),[225,228,240] and $[(trispicMeen)Fe^{III}(\eta^1\text{-}OOH)]^{2+}$ (**47**, Figure 33). The most thoroughly studied side-on peroxide is $[Fe^{III}\text{-}(EDTA)(\eta^2\text{-}O_2)]^{3-}$.[234] Another example of side-on peroxides is $[Fe^{III}(porphyrin)(\eta^2\text{-}O_2)]$.[241,242] Both Que and Girerd have shown that when ligated by nitrogen ligands, a side-on ferric peroxide will convert to end-on ferric hydroperoxide species upon protonation.[84,225,226,235,236,238] In both examples, the side-on peroxide (**44** and **46**; Figure 33) is $S = {}^5/_2$, whereas the end-on hydroperoxide (**45** and **47**) is $S = {}^1/_2$. The ν_{O-O} stretching frequencies of these side-on peroxides (827 (**44**) and 819 cm^{-1} (**46**)) are at higher energies than those of the corresponding end-on hydroperoxides (790 (**45**) and 796 cm^{-1} (**47**)). The ν_{Fe-O} stretch shifts from 495 to 632 cm^{-1} upon protonation of **44**, and from 470 to 617 cm^{-1} upon protonation of **46**. Thus, protonation results in a spin-state change (from $S = {}^5/_2$ to $S = {}^1/_2$) and, as predicted by Solomon,[227] weakening of the O−O bond (as reflected by the ν_{O-O} frequency). Given that two protons are added to the reduced peroxide product of SOR during catalysis, it is likely that if a side-on peroxide forms in wild type SOR, it probably converts to an end-on hydroperoxide prior to the release of H_2O_2 product.

None of the synthetic complexes described above (**44**−**47**) contain thiolate ligands. An obvious question in relation to SOR concerns how a thiolate sulfur ligand would affect H_2O_2 formation and release. It has been suggested that the *trans*-thiolate provides a pathway for electron delivery to the iron site and labilizes the Fe−O bond, favoring peroxide release.[36] If the latter were true, then one would expect the thiolate to perturb the properties of end-on and side-on Fe(III)-peroxide species relative to systems lacking a thiolate. It is also possible that, in contrast to the nitrogen-ligated systems, a π-donor sulfur ligand would favor a high-spin $Fe^{III}-OOH$ species. A high-spin $Fe^{III}-OOH$ species would be predicted to have a fairly weak Fe−O bond, in contrast to a low-spin $Fe^{III}-OOH$ species. Another obvious question concerns the positioning of the sulfur ligand. Does the positioning of this thiolate trans to the peroxide help to labilize the Fe−O bond? These are all questions that could be addressed with synthetic thiolate-ligated SOR models.

Halfen and co-workers have synthetically modeled the square pyramidal structure of reduced SOR using a pyridyl appended diazacyclooctane ligand (L^8py_2; Figure 35).[154] Aromatic thiolates (SAr = SC_6H_4-*p*-CH_3, SC_6H_4-*m*-CH_3, and SC_6H_{11}) coordinate to the apical position of reduced, high-spin ($S = 2$) $[(L^8py_2)\text{-}Fe^{II}(SAr)]^+$ (**48**; Figure 35), trans to an open coordination site. Oxidation of all three of these thiolate-ligated derivatives of **48** was found to be irreversible and results in the formation of disulfides.[154]

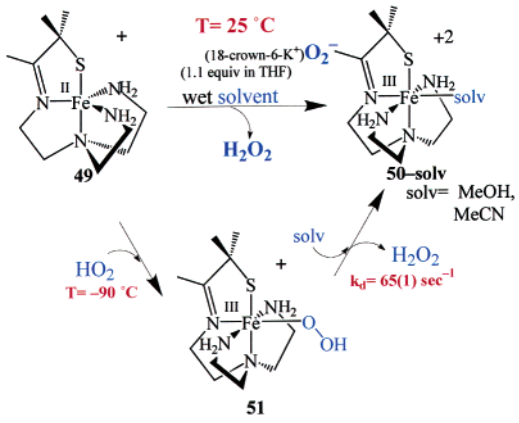

Figure 36. Reaction of five-coordinate, thiolate-ligated $[Fe^{II}(S^{Me_2}N_4(tren))]^+$ (**49**) with superoxide to afford solvent-ligated $[Fe^{III}(S^{Me_2}N_4(tren))(solv)]^{2+}$ (**50**) via a peroxide-bound intermediate $[Fe^{III}(S^{Me_2}N_4(tren))(OOH)]^+$ (**51**).

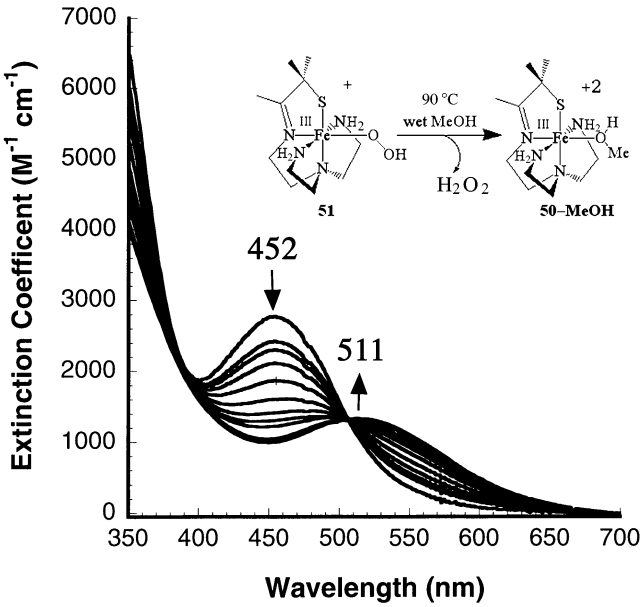

Figure 37. Electronic absorption spectrum showing that $[Fe^{III}(S^{Me_2}N_4(tren))(OOH)]^+$ (**51**; λ_{max} = 452(2780) nm), generated by adding 1.1 equiv of $(18\text{-crown-6-K}^+)O_2^-$ to $[Fe^{II}(S^{Me_2}N_4(tren)]^+$ (**49**) at −90 °C in MeOH/THF, cleanly converts to $[Fe^{III}(S^{Me_2}N_4(tren)(OMe)]^+$ (**50**-OMe; λ_{max} = 511-(1765) nm).

In 2001, Shearer and Kovacs showed that when the thiolate ligand is incorporated into a multidentate ligand, biomimetic SOR reactivity is observed, even if the thiolate is coordinated cis, as opposed to trans, to the open coordination site.[152,241] Five-coordinate, thiolate-ligated $[Fe^{II}(S^{Me_2}N_4(tren))]^+$ (**49**; Figure 36) reacts with superoxide (solubilized as an 18-crown-6-K^+ salt in THF) to afford H_2O_2 and solvent-ligated $[Fe^{III}(S^{Me_2}N_4(tren))(solv)]^{2+}$ (**50**; solv = MeCN or MeOH).[241] In MeCN, trace amounts of water serve as the proton source. In rigorously dried MeCN, **49** does not react with superoxide. At low temperatures (≤90 °C), a transient peroxide intermediate, $[Fe^{III}(S^{Me_2}N_4(tren)(OOH))]^+$ (**51**), is detected by electronic absorption (Figure 37), EPR, IR (Figure 38), and XAS spectroscopies. Peroxide intermediate **51** is low-spin ($S = {}^1/_2$; $g_\perp = 2.14$, $g_\parallel = 1.97$), displays a charge-transfer band at 452(2780 M^{-1} cm^{-1}) nm, and cleanly converts to intermediate-spin ($S = {}^3/_2$), methoxide-

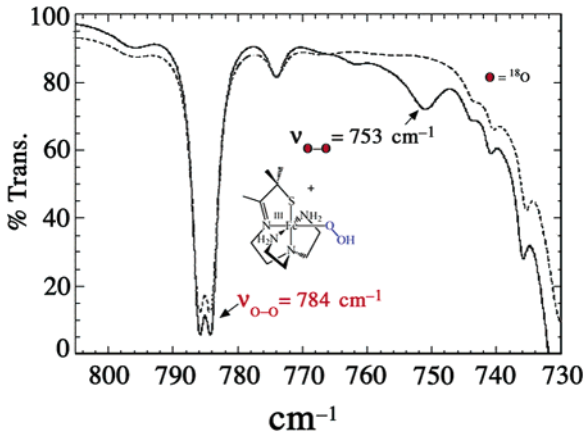

Figure 38. Low-temperature IR spectrum of $[Fe^{III}(S^{Me_2}N_4(tren))(OOH)]^+$ (**51**) formed via the addition of100% $^{16}O_2^-$ (---) or a 23.28% $^{18}O_2^-/^{16}O_2^-$ mixture (—) to **49** in wet acetone at −70 °C.

bound $[Fe^{III}(S^{Me_2}N_4(tren))(OMe)]^+$ (**50**-OMe) at low temperatures.[152] Peroxide is released from $[Fe^{III}(S^{Me_2}N_4(tren)(OOH))]^+$ (**51**) at a rate of 65(1) s^{-1} (at 298 K), a rate that is comparable to that of the SOR enzyme.[30−32,38,39,73] Peroxide-bound **51** displays a Fermi doublet in the IR (Figure 38) at 788 and 781 cm^{-1} which collapses to a singlet at 784 cm^{-1} upon deuteration.[152] A new ν_{O-O} stretch is observed at 752 cm^{-1} in the reaction between isotopically labeled $^{18}O_2^-$ and $[Fe^{II}(S^{Me_2}N_4(tren))]^+$ (**49**), confirming the ν_{O-O} assignment (Figure 38). This shift of 31 cm^{-1} is close to that predicted (44 cm^{-1}) for a diatomic oxygen species. Fits to the EXAFS data for **51** required a new short Fe−O bond at 1.86(3) Å that is not present in either the Fe^{II} precursor **49** or the MeO^--bound product **50**-OMe. Addition of an outer-sphere oxygen at 2.79(6) Å improved these fits slightly.[152] The small Debye−Waller factor associated with this outer-sphere oxygen suggests that this oxygen is highly ordered, possibly due to H-bonding between the hydroperoxide and the *cis*-thiolate sulfur. The XANES spectrum is consistent with a six-coordinate oxidized Fe^{III} intermediate. Together these data imply that, like the enzyme, oxidation of **49** proceeds via an inner-sphere electron-transfer pathway to afford an end-on $Fe^{III}(\eta^1 0-OOH)$ intermediate, $[Fe^{III}(S^{Me_2}N_4(tren)(OOH))]^+$ (**51**).

Cyanide, azide, and acetate all bind to $[Fe^{III}(S^{Me_2}N_4(tren))(MeCN)]^{2+}$ (**50**-MeCN) to afford models for the CN^--inhibited, N_3^--bound, and Glu-bound resting state of SOR (Figure 39).[153] Cyanide and azide do not bind to reduced **49**, on the other hand, and do not prevent **49** from stoichiometrically reducing superoxide to afford H_2O_2. Azide- and acetate-coordinated $[Fe^{III}(S^{Me_2}N_4(tren))(N_3)]^+$ (**52**) and $[Fe^{III}(S^{Me_2}N_4(tren))(OAc)]^+$ (**53**) each possess an $S = {}^1/_2$ ground state with a thermally accessible higher spin-state.[153] Cyanide-bound $[Fe^{III}(S^{Me_2}N_4(tren))(CN)]^+$ (**54**), on the other hand, is $S = {}^1/_2$ ($g_\perp = 2.13$, $g_\parallel = 2.00$) over the entire temperature range (2−300 K) examined. Cyanide also dramatically alters the magnetic properties of SOR: N_3-SOR and Glu-SOR SOR are high-spin ($S = {}^5/_2$), whereas CN-SOR is low-spin ($S = {}^1/_2$). These differences in spin-state are not surprising, given the differences in ligand-field strengths of N_3^- vs RCO_2^-

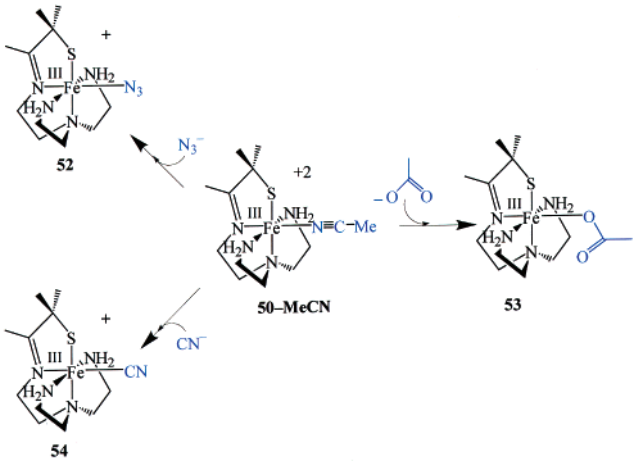

Figure 39. Synthetic analogues of cyanide-inhibited superoxide reductase (SOR), azide-ligated SOR, and the Glu-bound resting state of SOR.

vs CN^-. The redox properties of these model complexes are also dramatically altered by cyanide. Azide- and OAc-ligated **52** and **53** are reduced at similar potentials of −410 and −335 mV (vs SCE), respectively, whereas CN-ligated **54** is reduced at a much more anodic potential of −805 mV vs SCE. *If cyanide were to cause the redox potential of SOR to shift by approximately the same amount (−470 mV), then the reduction potential of the catalytic iron center (center II)*[23] *would fall well below those of its biological reductants* (center I, −236 mV vs SCE, and rubredoxin, reported range −191 to −291 mV vs SCE)). *Thus, cyanide would prevent the enzyme from turning over by preventing the reduced, catalytically active* Fe^{2+} *SOR state from being regenerated*. Cyanide inhibits superoxide dismutase in a similar manner, by preventing the Fe^{2+} state from being regenerated.[242] A possible explanation for this dramatic shift in potential upon CN^- binding is apparent when one considers that redox potentials reflect the relative stability of a metal complex in two different oxidation states. Reduction of Fe^{III}−CN involves a spin-state change, from low-spin Fe^{III}−CN containing no populated antibonding orbitals to high-spin Fe^{II} containing two antibonding electrons. With the azide and acetate derivatives, there would be much less loss in stability because the six-coordinate complexes start out with antibonding electrons. Given that electron transfer plays a prominent role in SOR chemistry, it is likely that SOR inhibition occurs by interfering with these redox processes as well.

4. Perspective

Despite the many challenges, much progress has been made in an attempt to determine the roles played by cysteinate sulfur ligands in promoting biological non-heme iron enzyme function. The molecular-level details regarding metalloprotein function are typically revealed using several complementary lines of study, at the interface of chemistry, biology, and physics.[137,138] As illustrated by the examples described in this review, small molecular analogues reproducing either key spectroscopic features or reactivity of metalloenzymes such as nitrile hydratase (NHase) and superoxide reductase (SOR) have helped to reveal details regarding the active site structure in relation to function and possible reaction mechanisms. When at least two thiolate sulfurs and either imine or amide ligands are incorporated into the coordination sphere, the low ($S = {}^1/_2$) spin-state of Fe^{III} is favored. This coordination environment also stabilizes iron in the 3+ oxidation state, making it redox inactive. The Lewis acidity of the metal ion is significantly decreased by replacing neutral imines with anionic carboxamides, and increased via oxygenation of the coordinated sulfurs. A systematic study which correlates the reactivity of thiolate-ligated Fe^{III}−N≡CR and Fe^{III}−OH species with ligand environment, spin-state, and the presence or absence of oxygenated sulfurs is required if we wish to fully understand how the structure of NHase contributes to its function. Experiments correlating NHase activity with the presence of $\nu_{S=O}$ vibrational stretches, or the observation of oxygenated sulfurs by S-XAS, would allow one to defintively determine whether both oxygenated sulfurs are required for activity. Studies of this nature have yet to be reported. Whether all of the reaction chemistry promoted by NHase takes place at a singly oxygenated sulfenate ligand also needs to be explored.

Despite their vastly different reactivities, nitrile hydratase (NHase) and superoxide reductase (SOR) have in common a non-heme iron active site containing a cysteinate sulfur trans to a "substrate binding site". The trans positioning of this sulfur has been proposed to play an important role in promoting the chemistry that occurs at these sites. As illustrated by the examples described in this review, the trans-labilizing effect of a coordinated sulfur ligand can be used to increase metal-bound product dissociation rates by several orders of magnitude, making an otherwise inert metal ion, such as the Co^{III} ion of NHase, reactive. With SOR, a biomimetic model was shown to promote SOR chemistry, despite the positioning of the thiolate sulfur cis, as opposed to trans, to the peroxide.[152] This suggests that a *trans*-thiolate may not be necessary to promote SOR function. In the heme iron enzyme cytochrome P450, which structurally resembles SOR, the trans cysteinate sulfur has been proposed to play an important role in promoting O−O bond cleavage.[51,67,68] How this O−O bond-cleaving chemistry is avoided with SOR remains to be determined. It is likely that the spin-state of the intermediate peroxide plays an important role in determining whether the Fe−O or O−O bond cleaves. Whether the peroxide intermediate that forms during catalysis by wild-type SOR is high-spin or low-spin remains to be determined. If such an intermediate can be detected in wild-type SOR, then a double-labeling experiment involving $^{16}O-^{18}O^-$ should be carried out in order to conclusively determine whether this intermediate contains an end-on or side-on peroxide. If we wish to fully understand how the electronic structure of SOR contributes to its function, then a systematic study correlating Fe−O (vs O−O) bond-cleaving properties with spin-state and the positioning of a thiolate sulfur (cis vs trans relative to the peroxide) is needed. Not enough

BATCH: cr80a25 USER: slr69 DIV: @xyv04/data1/CLS_pj/GRP_cr/JOB_i80/DIV_cr020619e DATE: January 2, 2004

is known about the chemistry of thiolate-ligated iron peroxides at this point to predict these properties.

5. References

(1) Kappock, T. J.; Caradonna, J. P. *Chem. Rev.* **1996**, *96*, 2659.
(2) Tomchick, D. R.; Phan, P.; Cymborowski, M.; Minor, W.; Holman, T. R. *Biochemistry* **2001**, *40*, 7509.
(3) Stubbe, J.; Riggs-Gelasco P. *Trends Biol. Sci.* **1998**, *23*, 438.
(4) Que, L., Jr.; Ho, R. Y. N. *Chem. Rev.* **1996**, *96*, 2607.
(5) Solomon, E. I.; Brunold, T. C.; Davis, M. I.; Kemsley, J. N.; Lee, S.; Lehnert, N.; Neese, F.; Skulan, A. J.; Yang, Y.; Ahou, J. *Chem. Rev.* **2000**, *100*, 235.
(6) Que, L., Jr. *Nature Struct. Biol.* **2000**, *7*, 182.
(7) Karlsson, A.; Parales, J. V.; Parales, R. E.; Gibson, D. T.; Eklund, H.; Ramaswamy, S. *Science* **2003**, *299*, 1039.
(8) Kovacs, J. A. *Science* **2003**, *299*, 1024.
(9) Rohde, J.-U.; In, J.-H.; Lim, M. H.; Brennessel, W. W.; Bukowski, M. R.; Stubna, A.; Munck, E.; Nam, W.; Que, L., Jr. *Science* **2003**, *299*, 1037.
(10) Costas, M. M., M. P.; Jensen, M. P.; Que, L., Jr. *Chem. Rev.* **2004**, in press.
(11) Shilov, A. E. Shulpin, G. B. *Chem. Rev.* **1997**, *97*, 2879.
(12) Nelson, M. J. *J. Am. Chem. Soc.* **1988**, *110*, 2985.
(13) Roth, J. P.; Mayer, J. M. *Inorg. Chem.* **1999**, *38*, 2760.
(14) Mayer, J. M. *Acc. Chem. Res.* **1998**, *31*, 441.
(15) Gupta, R.; Borvik, A. S. *J. Am. Chem. Soc.* **2003**, *125*, 13234.
(16) Jonas, R. T.; Stack, T. D. P. *J. Am. Chem. Soc.* **1997**, *119*, 8566.
(17) Noguchi, T.; Hoshino, M.; Tsujimura, M.; Odaka, M.; Inoue, Y.; Endo, I. *Biochemistry* **1996**, *35*, 16777.
(18) Brennan, B. A.; Jin, H.; Chase, D. B.; Turner, I. M.; Buck, C.; Scarrow, R. C.; Gurbiel, R.; Doan, P.; Hoffman, B. M.; Nelson, M. J. *J. Inorg. Biochem.* **1993**, *51*, 374.
(19) Brennan, B. A.; Alms, G.; Scarrow, R. C. *J. Am. Chem. Soc.* **1996**, *118*, 9194.
(20) Nagasawa, T.; Nanba, H.; Ryuno, K.; Takeuchi, K.; Yamada, H. *Eur. J. Biochem.* **1987**, *162*, 691.
(21) Nelson, M. J.; Jin, H.; Turner, I. M., Jr.; Grove, G.; Scarrow, R. C.; Brennan, B. A.; Que, L., Jr. *J. Am. Chem. Soc.* **1991**, *113*, 7072.
(22) Scarrow, R. C.; Brennan, B. A.; Nelson, M. J. *Biochemistry* **1996**, *35*, 10078.
(23) Brennan, B. A.; Cummings, J. G.; Chase, D. B.; Turner, I. M., Jr.; Nelson, M. J. *Biochemistry* **1996**, *35*, 10068.
(24) Scarrow, R. C.; Strickler, B.; Ellison, J. J.; Shoner, S. C.; Kovacs, J. A.; Cummings, J. G.; Nelson, M. J. *J. Am. Chem. Soc.* **1998**, *120*, 9237.
(25) Huang, W.; Jia, J.; Cummings, J.; Nelson, M.; Schneider, G.; Lindqvist, Y. *Structure* **1997**, *5*, 691.
(26) Nagashima, S.; Nakasako, M.; Naoshi, D.; Tsujimura, M.; Takio, K.; Odaka, M.; Yohda, M.; Kamiya, N.; Endo, I. *Nat. Struct.Biol.* **1998**, *5*, 347.
(27) Kobayashi, M.; Shimizu, S. *Nat. Biotechnol.* **1998**, *16*, 733.
(28) Endo, I.; Nojiri, M.; Tsujimura, M.; Nakasako, M.; Nagashima, S.; Yohda, M.; Odaka, M. *J. Inorg. Biochem.* **2001**, *83*, 247.
(29) Mathe, C.; Mattioli, T. A.; Horner, O.; Lombard, M.; Latour, J.-M.; Fontecave, M.; Niviere, V. *J. Am. Chem. Soc.* **2002**, *124*, 4966.
(30) Coulter, E. D.; Lombard, M.; Houee-Levin, C.; Touati, D.; Fontecave, M.; Niviere, V. *Biochemistry* **2001**, *40*, 5032.
(31) Coulter, E. D.; Emerson, J. P.; Kurtz, D. M., Jr.; Cabelli, D. E. *J. Am. Chem. Soc.* **2000**, *122*, 11555.
(32) Abreu, I. A.; Saraiva, L. M.; Carita, J.; Huber, H.; Stetter, K. O.; Cabelli, D.; Teixeira, M. *Mol. Microbiol.* **2000**, *38*, 322.
(33) Jenney, F. E., Jr.; Verhagen, M. F. J. M.; Cui, X.; Adams, M. W. W. *Science* **1999**, *286*, 306.
(34) Yeh, A. P.; Hu, Y.; Jenney, F. E., Jr.; Adams, M. W. W.; Rees, D. C. *Biochemistry* **2000**, *39*, 2499.
(35) Kurtz, D. M.; Coulter, E. D. *J. Biol. Inorg. Chem.* **2002**, *7*, 653.
(36) Clay, M. D.; Jenney, F. E., Jr.; Hagedoorn, P. L.; George, G. N.; Adams, M. W. W.; Johnson, M. K. *J. Am. Chem. Soc.* **2002**, *124*, 788.
(37) Clay, M.; Cosper, C. A.; Jenney, F. E., Jr.; Adams, M. W. W.; Johnson, M. K. *Proc. Natl. Acad. Sci., U.S.A.* **2003**, *100*, 3796.
(38) Silaghi-Dumitrescu, R.; Silaghi-Dumitrescu, I.; Coulter, E. D.; Kurtz, D. M., Jr. *Inorg. Chem.* **2003**, *42*, 446.
(39) Niviere, V.; Lombard, M.; Fontecave, M.; Houee-Levin, C. *FEBS Lett.* **2001**, *497*, 171.
(40) Lumppio, H. L.; Shenvi, N. V.; Summers, A. O.; Voordouw, G.; Kurtz, D. M., Jr. *J. Bacteriol.* **2001**, *183*, 101.
(41) Ascenso, C.; Rusnak, F.; Cabrito, I.; Lima, M. J.; Naylor, S.; Moura, I.; Moura, J. J. G. *J. Biol. Inorg. Chem.* **2000**, *5*, 720.
(42) Jovanovic, T.; Ascenso, C.; Hazlett, K. R. O.; Sikkink, R.; Krebs, C.; Litwiller, R.; Benson, L. M.; Moura, I.; Moura, J. J. G.; Radolf, J. D. *J. Biol. Chem.* **2000**, *275*, 28439.
(43) Meinnel, T.; Blanquet, S.; Dardel, F. *J. Mol. Biol.* **1996**, *262*, 375.
(44) Rajagopalan, P. T. R.; Yu, X. C.; Pei, D. *J. Am. Chem. Soc.* **1997**, *119*, 12418.
(45) Chang, S.; Karambelkar, V. V.; diTargiani, R. C.; Goldberg, D. P. *Inorg. Chem.* **2001**, *40*, 194.
(46) Becker, A.; Schlichting, I.; Kabsch, W.; Groche, D.; Schultz, S.; Wagner, A. F. V. *Nat. Struct. Biol.* **1998**, *5*, 1053.
(47) Jin, H.; Turner, I. M., Jr.; Nelson, M. J.; Gurbiel, R. J.; Doan, P. E.; Hoffman, B. M. *J. Am. Chem. Soc.* **1993**, *115*, 5290.
(48) Odaka, M.; Fujii, K.; Hoshino, M.; Noguchi, T.; Tsujimura, M.; Nagashima, S.; Yohada, N.; Nagamune, T.; Inoue, I.; Endo, I. *J. Am. Chem. Soc.* **1997**, *119*, 3785.
(49) Mayer, S. M.; Lawson, D. M.; Gormal, C. A.; Roe, S. M.; Smith, B. E. *J. Mol. Biol.* **1999**, *292*, 871.
(50) Doukov, T. I.; Iverson, T. M.; Servalli, J.; Ragsdale, S. W.; Drennan, C. L. *Science* **2002**, *298*, 567.
(51) Loew, G. H.; Harris, D. L. *Chem. Rev.* **2000**, *100*, 407.
(52) Sugiura, Y.; Kuwahara, J.; Nagasawa, T.; Yamada, H. *J. Am. Chem. Soc.* **1987**, *109*, 5848.
(53) Lombard, M.; Fontecave, M.; Touati, D.; Niviere, V. *J. Biol. Chem.* **2000**, *275*, 115.
(54) Noveron, J. C.; Olmstead, M. M.; Mascharak, P. K. *Inorg. Chem.* **1998**, *37*, 1138.
(55) Patra, A. K.; Ray, M.; Mukherjee, R. *Inorg. Chem.* **2000**, *39*, 652.
(56) Collins, T. J. *Acc. Chem. Res.* **1994**, *27*, 279.
(57) Margerum, D. W. *Pure Appl. Chem.* **1983**, *55*, 23.
(58) Brewer, J. C.; Collins, T. J.; Smith, M. R.; Santasiero, B. D. *J. Am. Chem. Soc.* **1988**, *110*, 423.
(59) Glaser, T.; Hedman, B.; Hodgson, K. O.; Solomon, E. I. *Acc. Chem. Res.* **2000**, *33*, 859.
(60) Randall, D. W.; George, S. D.; Hedman, B.; Hodgson, K. O.; Fujisawa, K.; Solomon, E. I. *J. Am. Chem. Soc.* **2000**, *122*, 11620.
(61) George, S. D.; Metz, M.; Szilagyi, R. K.; Wang, H.; Cramer, S. P.; Lu, Y.; Tolman, W. B.; Hedman, B.; Hodgson, K. O.; Solomon, E. I. *J. Am. Chem. Soc.* **2001**, *123*, 5757.
(62) Lowery, M. D.; Guckert, J. A.; Gebhard, M. S.; Solomon, E. I. *J. Am. Chem. Soc.* **1993**, *115*, 3012.
(63) Shoner, S.; Barnhart, D.; Kovacs, J. A. *Inorg. Chem.* **1995**, *34*, 4517.
(64) Jackson, H. L.; Shoner, S. C.; Rittenberg, D.; Cowen, J. A.; Lovell, S.; Barnhart, D.; Kovacs, J. A. *Inorg. Chem.* **2001**, *40*, 1646.
(65) Ellison, J. J.; Nienstedt, A.; Shoner, S. C.; Barnhart, D.; Cowen, J. A.; Kovacs, J. A. *J. Am. Chem. Soc.* **1998**, *120*, 5691.
(66) Sono, M.; Roach, M. P.; Coulter, E. D.; Dawson, J. H. *Chem. Rev.* **1996**, *96*, 2841.
(67) Meunier, B.; Bernadou, J. *Struct. Bonding* **2000**, *97*, 1.
(68) Auclair, K.; Moe1nne-Loccoz, P.; Ortiz de Montellano, P. R. *J. Am. Chem. Soc.* **2001**, *123*, 4877.
(69) Heinrich, L.; Mary-Verla, A.; Li, Y.; Vaissermann, J.; Chottard, J.-C. *Eur. J. Inorg. Chem.* **2001**, 2203.
(70) Lydon, J. D.; Deutsch, E. *Inorg. Chem.* **1982**, *21*, 3180.
(71) Adzamili, I. K.; Libson, K.; Lydon, J. D.; Elder, R. C.; Deutsch, E. *Inorg. Chem.* **1979**, *18*, 303.
(72) Banerjee, A.; Sharma, R.; Banerjee, U. C. *Appl. Microbiol. Biotech.* **2002**, *60*, 33.
(73) Kurtz, D. M., Jr.; Coulter, E. D. *Chemtracts* **2001**, *14*, 407.
(74) Adams, M. W. W.; Jenney, F. E., Jr.; Clay, M. D.; Johnson, M. K. *J. Biol. Inorg. Chem.* **2002**, *7*, 647.
(75) Yamada, H.; Shimizu, S.; Kobayashi, M. *The Chemical Record* **2001**, *1*, 152.
(76) Auchere, F.; Rusnak, F. *J. Biol. Inorg. Chem.* **2002**, *7*, 664.
(77) Endo, I.; Odaka, M.; Yohda, M. *Trends Biotechnol.* **1999**, *17*, 244.
(78) Mascharak, P. K. *Coord. Chem.* **2002**, *225*, 201.
(79) Artaud, I.; Chatel, S.; Chauvin, A. S.; Bonnet, D.; Kopf, M. A.; Leduc, P. *Coord. Chem. Rev.* **1999**, *190−192*, 577.
(80) Baik, M.-H.; Newcomb, M.; Friesner, R. A.; Lippard, S. J. *Chem. Rev.* **2003**, *103*, 2385.
(81) Feig, A. L.; Lippard. S. J. *Chem. Rev.* **1994**, *94*, 759.
(82) Girerd, J.-J.; B., F.; Simaan, A. J. *Struct. Bonding* **2000**, *97*, 145.
(83) Waller, B. J.; Lipscomb, J. D. *Chem. Rev.* **1996**, *96*, 2625.
(84) Rosenzweig, A. C.; Lippard, S. J. *Acc. Chem. Res.* **1994**, *27*, 229.
(85) Nagasawa, T.; Ryuno, K.; Yamada, H. *Biochem. Biophys. Res. Commun.* **1986**, *139*, 1305.
(86) Tsujimura, M.; Odaka, M.; Nagashma, S.; Yohda, M.; Endo, I. *J. Biochem.* **1996**, *119*, 407.
(87) Honda, J.; Kandori, H.; Okada, T.; Nagamune, T.; Shichida, Y.; Sasabe, H.; Endo, I. *Biochemistry* **1994**, *33*, 3577.
(88) Maddrell, S. J.; Turner, N. J.; Crosby, J. *Tetrahedron Lett.* **1996**, *37*, 6001.
(89) Nagamune, T.; Honda, J.; Kobayashi, Y.; Sasabe, H.; Endo, I.; Ambe, F. *Hyperfine Interact.* **1992**, *71*, 1271.
(90) Noguchi, T.; Honda, J.; Nagamune, T.; Sasabe, H.; Inoue, Y.; Endo, I. *FEBS Lett.* **1995**, *358*, 9.
(91) Odaka, M.; Noguchi, T.; Nagashma, S.; Yohda, M.; Yabuki, S.; Hoshino, M,; Inoue, Y.; Endo, I. *Biochem. Biophys. Res. Commun.* **1996**, *221*, 146.
(92) Tsujimura, M.; Dohmae, N.; Endo, I. *J. Biol. Chem.* **1997**, *272*, 29454.
(93) Kobayashi, M.; Nagasawa, T.; Yamada, H. *Tibtech* **1992**, *10*, 402.

BATCH: cr80a25 USER: slr69 DIV: @xyv04/data1/CLS_pj/GRP_cr/JOB_i80/DIV_cr020619e DATE: January 2, 2004

(94) Nagasawa, T.; Takeuchi, K.; Yamada, H. *Eur. J. Biochem.* **1991**, *196*, 581.
(95) Eklund, H.; Branden, C.-I. *Zinc Enzymes*; Wiley: New York, 1983.
(96) Coleman, J. E. *Curr. Opin. Chem. Biol.* **1998**, *2*, 222.
(97) Meyerstein, D.; Goldstein, S. *Acc. Chem. Res.* **1999**, *32*, 547.
(98) Hlavaty, J. J.; Benner, J. S.; Hornstra, L. J.; Schildkraut, I. *Biochemistry* **2000**, *39*, 3097.
(99) Murakami, T.; Nojiri, M.; Nakayama, H.; Odaka, M.; Yohda, M.; Dohmae, N.; Takio, K.; Nagamune, T.; Endo, I. *Protein Sci.* **2000**, *9*, 1024.
(100) Kobayashi, M.; Nishiyama, M.; Nagasawa, T.; Horinouchi, S.; Beppu, T.; Yamada, H. *Biochim. Biophys. Acta* **1991**, *1129*, 23.
(101) Miyanaga, A.; Fushinobu, S.; Ito, K.; Wakagi, T. *Biochem. Biophys. Res. Commun.* **2001**, *288*, 1169.
(102) Nojiri, M.; Yohda, M.; Odaka, M.; Matsushita, Y.; Tsujimura, M.; Yoshida, T.; Dohmae, N.; Takio, K.; Endo, I. *J. Biochem. (Tokyo)* **1999**, *125*, 696.
(103) Allison, W. S. *Acc. Chem. Res.* **1976**, *9*, 293.
(104) Tsujimura, M.; Odaka, M.; Nakayama, H.; Dohmae, N.; Koshino, H.; Asami, T.; Hoshino, M.; Takio, K.; Yoshida, S.; Maeda, M.; Endo, I. *J. Am. Chem. Soc.* **2003**, *125*, 11532.
(105) Boone, A. J.; Cory, M. G.; Scott, M. J.; Zerner, M. C.; Richards, N. G. J. *Inorg. Chem.* **2001**, *40*, 1837.
(106) Piersma, S. R.; Nojiri, M.; Tsujimura, M.; Noguchi, T.; Odaka, M.; Yohda, M.; Inoue, Y.; Endo, I. *J. Inorg. Biochem.* **2000**, *80*, 283.
(107) Maelia, L. E.; Millar, M.; Koch, S. A. *Inorg. Chem.* **1992**, *31*, 4594.
(108) Millar, M.; Lee, J. F.; Fikar, R. *Inorg. Chim. Acta* **1996**, *243*, 333.
(109) Herskovitz, T.; Depamphilis, B. V.; Gillum, W. O.; Holm, R. H. *Inorg. Chem.* **1975**, *14*, 1426.
(110) Tsai, R.; Yu, C. A.; Gunsalus, I. C.; Peisach, J.; Blumberg, W.; Orme-Johnson, W. H.; Beinert, H. *Proc. Natl. Acad. Sci. U.S.A.* **1970**, *66*, 1157.
(111) Bonnet, D.; Artaud, I.; Moali, C..; Petre, D.; Mansuy, D. *FEBS Lett.* **1997**, *409*, 216.
(112) Nowak, W.; Ohtusuka, Y.; Hasegawa, J.; Nakatsuji, *Int. J. Quantum Chem.* **2002**, *90*, 1174.
(113) Popescu, V.-C.; Fox, B. G.; Sanakis, Y.; Cummings, J. G.; Turner, I. M., Jr.; Nelson, M. J. *Biochemistry* **2001**, *40*, 7984.
(114) Versari, A.; Menard, R.; Lortie, R. *Biotechnol. Bioeng.* **2002**, *79*, 9.
(115) Zervos, C.; Cordes, E. H. *J. Org. Chem.* **1971**, *36*, 1661.
(116) Komeda, H.; Hori, U. Y.; Kobayashi, M.; Shimizu, *Proc. Natl. Acad. Sci. U.S.A.* **1996**, *93*, 10572.
(117) Novai da Rocha, Z.; Chiericato, G., Jr.; Tfouni, E. In *Electron-Transfer Reactions: Inorganic, Organometallic, and Biological Applications*; Isied, S. S., Ed.; ACS Advances in Chemistry Series 253; American Chemical Society: Washington, DC, 1997; p 297.
(118) Rabinovitch, B. S.; Winkler, C. A *Can. J. Res.* **1949**, *20B*, 185.
(119) Breslow, R.; Fairweather, R.; Keana, J. *J. Am. Chem. Soc.* **1967**, *89*, 2135.
(120) Balahura, R. J.; Cock, P.; Purcell, W. L. *J. Am. Chem. Soc.* **1974**, *96*, 2739.
(121) Kukushkin, V. Y.; Pombeiro, A. J. L. *Chem. Rev.* **2002**, *102*, 1771.
(122) Kato, Y.; Tsuda, T.; Asano, Y. *Eur. J. Biochem.* **1999**, *263*, 662.
(123) Alfani, F.; Cantarella, M.; Spera, A.; Viparelli, P. *J. Mol. Catal.* **2001**, *11*, 687.
(124) Tyler, L. A.; Noveron, J. C.; Olmstead, M. M.; Mascharak, P. K. *Inorg. Chem.* **2003**, *42*, 5751.
(125) Shearer, J.; Kung, I. Y.; Lovell, S.; Kaminsky, W.; Kovacs, J. A. *J. Am. Chem. Soc.* **2001**, *123*, 463.
(126) Shearer, J. Jackson, H. L.; Schweitzer, D.; Rittenberg, D. K.; Leavy, T. M.; Kaminsky, W.; Scarrow, R. C.; Kovacs, J. A. *J. Am. Chem. Soc.* **2002**, *124*, 11417.
(127) Zanella, A. W.; Ford, P. C. *Inorg. Chem.* **1975**, *14*, 42.
(128) Kim, J. H.; Britten, J.; Chin, J. *J. Am. Chem. Soc.* **1993**, *115*, 3618.
(129) Coleman, J. E. *J. Biol. Chem.* **1967**, *242*, 5212.
(130) Kaminskaia, N. V.; He, C.; Lippard, S. J. *Inorg. Chem.* **2000**, *39*, 3365.
(131) Bencini, A.; Berni, E.; Bianchi, A.; Fedi, V.; Giorgi, C.; Paoletti, P.; Valtancoli, B. *Inorg. Chem.* **1999**, *38*, 6323.
(132) Caulton, K. G. *Chemtracts−Inorg. Chem.* **1999**, *12*, 890.
(133) Nojiri, M.; Nakayama, H.; Odaka, M.; Yohda, M.; Takio, K.; Endo, I. *FEBS Lett.* **2000**, *465*, 173.
(134) Payne, M. S.; Wu, S.; Fallon, R. D.; Tudor, G.; Stieglitz, B.; Turner, I. M., Jr.; Nelson, M. J. *Biochemistry* **1997**, *36*, 5447.
(135) Pogorelova, T. E.; Ryabchenko, L. E.; Yanenko, A. S. *FEMS Microbiol. Lett.* **1996**, *144*, 191.
(136) Lippard, S. J.; Berg, J. M. *Principles of Bioinorganic Chemistry*; University Science: Mill Valley, CA, 1994.
(137) Halpern, J.; Raymond, K. N. *Proc. Natl. Acad. Sci. U.S.A.* **2003**, *100*, 3562.
(138) Gray, H. B. *Proc. Natl. Acad. Sci. U.S.A.* **2003**, *100*, 3563.
(139) Holm, R. H.; Kennepohl, P.; Solomon, E. I. *Chem. Rev.* **1996**, *96*, 2239.
(140) Solomon, E. I. *Inorg. Chem.* **2001**, *40*, 3656.
(141) Hoffman, B. M. *Accounts. Chem. Res.* **2003**, *36*, 522.
(142) Munck, E. In *Aspects of ^{57}Fe Mossbauer Spectrscopy*; Que, L., Jr., Ed.; 2000.
(143) Ibers, J. A.; Holm, R. H. *Science* **1980**, *209*, 223.
(144) For example, it was only after synthetic analogues of hemerythrin were available for molecular-level detailed study that it became obvious that a proton, responsible for both stabilizing the peroxide intermediate and facilitating its formation, was present in the deoxy state, sitting on the μ-oxo.
(145) Stenkamp, R. E. *Chem. Rev.* **1994**, *94*, 715.
(146) Hartman, J. R.; Rardin, R. L.; Chaudhuri, P.; Pohl, K.; Wieghardt, K.; Nuber, B.; Weiss, J.;. Papaefthymiou, G. C.; Frankel, R. B.; Lippard, Stephen J. *J. Am. Chem. Soc.* **1987**, *109*, 7387.
(147) Chaudhuri, P.; Wieghardt, K.; Nuber, B.; Weiss, J. *Angew. Chem.* **1985**, *97*, 774.
(148) Hagen, K. S.; Holm, R. H. *J. Am. Chem. Soc.* **1982**, *104*, 5496.
(149) Corwin, D. T., Jr.; Gruff, E. S.; Koch, S. A. *J. Chem. Soc., Chem. Commun.* **1987**, *13*, 966.
(150) Kung, I.; Schweitzer, D.; Shearer, J.; Taylor, W. D.; Jackson, H. L.; Lovell, S.; Kovacs, J. A. *J. Am. Chem. Soc.* **2000**, *122*, 8299.
(151) Schweitzer, D.; Ellison, J. J.; Shoner, S. C.; Lovell, S.; Kovacs, J. A. *J. Am. Chem. Soc.* **1998**, *120*, 10996.
(152) Shearer, J.; Scarrow, R. C.; Kovacs, J. A. *J. Am. Chem. Soc.* **2002**, *124*, 11709.
(153) Shearer, J.; Fitch, S. B.; Kaminsky, W.; Benedict, J.; Scarrow, R. C.; Kovacs, J. A. *Proc. Natl. Acad. Sci. U.S.A.* **2003**, *100*, 3671.
(154) Halfen, J. A.; Moore, H. L.; Fox, D. C. *Inorg. Chem.* **2002**, *41*, 3935.
(155) Grapperhaus, C. A.; Patra, A. K.; Mashuta, M. S. *Inorg. Chem.* **2002**, *41*, 1039.
(156) Beissel, T.; Buerger, K. S.; Voigt, G.; Wieghardt, K.; Butzlaff, C.; Trautwein, A. X. *Inorg. Chem.* **1993**, *32*, 124.
(157) Noveron, J. C.; Olmstead, M. M.; Mascharak, P. K. *J. Am. Chem. Soc.* **2001**, *123*, 3247.
(158) Tyler, L. A.; Noveron, J. C.; Olmstead, M. M.; Mascharak, P. K. *Inorg. Chem.* **1999**, *38*, 616.
(159) Noveron, J. C.; Olmstead, M. M.; Mascharak, P. K. *J. Am. Chem. Soc.* **1999**, *121*, 3553.
(160) Heinrich, L.; Li, Y.; Vaissermann, J.; Chottard, G.; Chottard, J.-C. *Angew. Chem., Int. Ed.* **1999**, *38*, 3526.
(161) Heinrich, L.; Li, Y.; Provost, K.; Michalowicz, A.; Vaissermann, J.; Chottard, J. C. *Inorg. Chim. Acta* **2001**, *318*, 117.
(162) Chatel, S.; Rat, M.; Dijols, S.; Leduc, P.; Tuchagues, J. P.; Mansuy, D.; Artaud, I. *J. Inorg. Biochem.* **2000**, *80*, 239.
(163) Rat, M.; Alves de Sousa, R.; Vaissermann, J.; Leduc, P.; Mansuy, D.; Artaud, I. *J. Inorg. Biochem.* **2001**, *84*, 207.
(164) Grapperhaus, C. A. L., M.; Patra, A. K.; Potuovic, S.; Kozlowski, P. M.; Zgierski, M. Z.; Mashuta, M. S. *Inorg. Chem.* **2003**, *42*, 4382.
(165) Nivorozhkin, A. L. U., A. I.; Bondarenko, G. I.; Antsyshkina, A. S.; Kurbatov, V. P.; Garnovskii, A. D.; Turta, C. I.; Brashoveanu, N. D. *J. Chem. Soc., Chem. Commun.* **1997**, 1711.
(166) Sakurai, H.; Tsuchiya, K.; Migita, K. *Inorg. Chem.* **1988**, *27*, 3879.
(167) Kennepohl, P.; Schweitzer, D.; Jackson, H. l.; Kovacs, J. A.; Solomon, E. I., manuscript in preparation.
(168) Solomon, E. I.; Baldwin, M. J.; Lowery, M. D. *Chem. Rev.* **1992**, *92*, 521.
(169) Fallon, G. D.; Gatehouse, B. M. *J. Chem. Soc., Dalton Trans.* **1975**, 1344.
(170) Schaffer, C. E.; Jorgensen, C. K. *J. Inorg. Nucl. Chem.* **1958**, *8*, 143.
(171) Grapperhaus, C. A.; Darensbourg, M. Y. *Acc. Chem. Res.* **1998**, *31*, 451.
(172) Buonomo, R. M.; Font, I.; Maguire, M. J.; Reibenspies, J. H.; Tuntulani, T.; Darensbourg, M. Y. *J. Am. Chem. Soc.* **1995**, *117*, 963.
(173) Farmer, P. J.; Solouki, T.; Mills, D. K.; Soma, T.; Russell, D. H.; Reibenspies, J. H.; Darensbourg, M. Y. *J. Am. Chem. Soc.* **1992**, *114*, 4601.
(174) Farmer, P. J.; Solouki, T.; Soma, T.; Russell, D. H.; Darensbourg, M. Y. *Inorg. Chem.* **1993**, *32*, 4171.
(175) Font, I.; Buonomo, R.; Reibenspies, J. H.; Darensbourg, M. Y. *Inorg. Chem.* **1993**, *32*, 5897.
(176) Farmer, P. J.; Verpeaux, J.-N.; Amatore, C.; Darensbourg, M. Y.; Musie, G. *J. Am. Chem. Soc.* **1994**, *116*, 9355.
(177) Galvez, C.; Ho, D. G.; Azpd, A.; Selke, M. *J. Am. Chem. Soc.* **2001**, *123*, 3381.
(178) Tyler, L. A.; Noveron, J. C.; Olmstead, M. M.; Mascharak, P. K. *Inorg. Chem.* **2000**, *39*, 357.
(179) Heinrich, L.; Li, Y.; Vaissermann, J.; Chottard, G.; Chottard, J.-C. *Angew. Chem., Int. Ed.* **1999**, *38*, 3526.
(180) Shearer, J.; Kung, I.; Lovell, S. Kovacs, J. A. *Inorg. Chem.* **2000**, *39*, 4998.
(181) Fikar, R.; Koch, S. A.; Millar, M. M. *Inorg. Chem.* **1985**, *24*, 3311.
(182) Krebs, C.; Pereira, A. S.; Tavares, P.; Huynh, B. H.; Schweitzer, D.; Ellison, J. J.; Kovacs, J. A., manuscript in preparation.

BATCH: cr80a25 USER: slr69 DIV: @xyv04/data1/CLS_pj/GRP_cr/JOB_i80/DIV_cr020619e DATE: January 2, 2004

(183) Scarrow, R. C.; Strickler, B. S.; Ellison, J. J.; Shoner, S. C.; Kovacs, J. A.; Cummings, J. G.; Nelson, M. J. *J. Am. Chem. Soc.* **1998**, *120*, 9237.
(184) Bui, K.; Maistracci, M.; Thiery, A.; Arnaud, A.; Galzy, P. *J. Appl. Bacteriol.* **1984**, *57*, 183.
(185) Fallon, R. D.; Stieglitz, B.; Turner, I., Jr. *Appl. Microbiol. Biotechnol.* **1997**, *47*, 156.
(186) Doan, P.; Nelson, M. J.; Jin, H.; Hoffman, B. M. *J. Am. Chem. Soc.* **1996**, *118*, 7014.
(187) Evans, D. R.; Reed, C. A. *J. Am. Chem. Soc.* **2000**, *122*, 4660.
(188) Almarsson, O.; Adalsteinsson, H.; Bruice, T. C. *J. Am. Chem. Soc.* **1995**, *117*, 4524.
(189) Kurtz, D. M., Jr. *Chem. Rev.* **1990**, *90*, 585.
(190) Caudle, M. T.; Caldwell, C. D.; Crumbliss, A. L. *Inorg. Chim. Acta* **1995**, *240*, 519.
(191) Ivanovic-Burmazovic, I.; Hamza, M. S. A.; van Eldik, R. *Inorg. Chem.* **2002**, *41*, 5150.
(192) Ogo, S.; Wada, S.; Watanabe, Y.; Iwase, M.; Wada, A.; Harata, M.; Jitsukawa, K.; Masuda, H.; Einaga, H. *Angew. Chem., Int. Ed.* **1998**, *37*, 2102.
(193) MacBeth, C. E.; Golombek, A. P.; Young, V. G., Jr.; Yang, C.; Kuczera, K.; Hendrich, M. P.; Borovik, A. S. *Science* **2000**, *289*, 938.
(194) Yeh, C.-Y.; Chang, C. J.; Nocera, D. G. *J. Am. Chem. Soc.* **2001**, *123*, 1513.
(195) Schweitzer, D. S., J.; Rittenberg, D. K.; Shoner, S. C.; Ellison, J. J.; Loloee, R.; Lovell, S.; Barnhart, D.; Kovacs, J. A. *Inorg. Chem* **2002**, *41*, 3128.
(196) Elder, R. C.; Kennard, G. J.; Payne, M. D.; Deutsch, E. *Inorg. Chem.* **1978**, *17*, 12.
(197) Buckingham, D. A.; Keene, F. R.; Sargeson, A. M. *J. Am. Chem. Soc.* **1973**, *95*, 5649.
(198) Balahura, R. J.; Cock, P.; Purcell, W. L. *J. Am. Chem. Soc.* **1974**, *96*, 2739.
(199) Gonzalez, G.; Moullet, B.; Martinez, M.; Merbach, A. E. *Inorg. Chem.* **1994**, *33*, 2330.
(200) Winkler, J. R.; Rice, S. F.; Gray, H. B. *Comments Inorg. Chem* **1981**, *1*, 47.
(201) Higgs, T. C.; Ji, D.; Czernuszewicz, R. S.; Matzanke, B. F.; Schunemann, V.; Trautwein, A. X.; Helliwell, M.; Ramirez, W.; Carrano, C. J *Inorg. Chem.* **1998**, *37*, 2383.
(202) Sawyer, D. T.; Valentine, J. S. *Acc. Chem. Res.* **1981**, *14*, 393.
(203) Liochev, S. I.; Fridovich, I. *J. Biol. Chem.* **1997**, *272*, 25573.
(204) Fridovich, I. *Acc. Chem. Res.* **1972**, *5*, 321.
(205) Otani, H.; Umemoto, M.; Kagawa, K.; Nakamura, Y.; Omoto, K.; Tanaka, K.; Sato, T.; Nonoyama, A.; Kagawa, T. *J. Surg. Res.* **1986**, *41*, 126.
(206) Fortunato, G.; Pastinese, A.; Intrieri, M.; Lofrano, M. M.; Bolletti Gaeta, G.; Censi, M. B.; Boccalatte, A.; Salvatore, F.; Sacchetti, L. *Clin. Biochem.* **1997**, *30*, 5569.
(207) Kocaturk, P. A.; Akbostanci, M. C.; Tan, F.; Kavas, G. O. *Pathophysiology* **2000**, *7*, 63.
(208) Ihara, Y.; Chuda, M.; Kuroda, S.; Hayabara, T. *J. Neurol. Sci.* **1999**, *170*, 90.
(209) De Leo, M. E.; Borrello, S.; Passantino, M.; Palazzotti, B.; Mordente, A.; Daniele, A.; Filippini, V.; Galeotti, T.; Masullo, C. *Neurosci. Lett.* **1998**, *250*, 173.
(210) Fernandes, M. A. S.; Santana, I.; Januario, C.; Cunha, L.; Oliveria, C. R. *Med. Sci. Res.* **1993**, *21*, 920.
(211) Marklund, S. L.; Adolfsson, R.; Gottfries, C. G.; Winblad, B. *J. Neurol. Sci.* **1985**, *67*, 319.
(212) Gogun, Y.; Sakurada, S.; Kimura, Y.; Nagumo, M. *J. Clin. Biochem. Nutr.* **1990**, *8*, 85.
(213) Buettner, G. R.; Oberley, L. W. *Oxygen Oxy-Radicals Chem. Biol., [Proc. Int. Conf.]* **1981**, 606.
(214) Coelho, A. V.; Matias, P.; Fulop, V.; Thompson, A.; Gonzalez, A.; Carrondo, M. A. *J. Biol. Inorg. Chem.* **1997**, *2*, 680.
(215) The former was characterized both in the oxidized ferric resting state and in the reduced catalytically active ferrous state, while the latter was characterized only in the oxidized ferric state. Partial photoreduction of the oxidized state occurs in the X-ray beam to afford mixtures of the reduced and oxidized states. Consequently, some of the oxidized state structures appeared to be five-coordinate.
(216) Fee, J. A.; McClune, G. J.; O'Neill, P.; Fielden, E. M. *Biochem. Biophys. Res. Commun.* **1981**, *100*, 377.
(217) Tavares, P.; Ravi, N.; Moura, J. J. G.; LeGall, J.; Huang, Y.-H.; Crouse, B. R.; Johnson, M. K.; Huynh, B. H.; Moura, I. *J. Biol. Chem.* **1994**, *269*, 10504.
(218) Abreu, I. A.; Xavier, A. V.; LeGall, J.; Cabelli, D.; Teixeira, M. *J. Biol. Inorg. Chem.* **2002**, *7*, 668.
(219) Chen, L.; Sharma, P.; LeGall, J.; Mariano, A. M.; Teixeira, M.; Xavier, A. V. *Eur. J. Biochem.* **1994**, *226*, 613.
(220) Burger, R. M. *Struct. Bonding* **2000**, *97*, 287.
(221) Ortiz de Montellano, P. R. *Acc. Chem. Res.* **1998**, *31*, 543.
(222) Wolfe, M. D.; Parales, J. V.; Gibson, D. T.; Lipscomb, J. D. *J. Biol. Chem.* **2001**, *276*, 1945.
(223) Roelfes, G.; Vrajmasu, V.; Chen, K.; Ho, R. Y. N.; Rohde, J.-U.; Zondervan, C.; Crois, R. M.; Schudde, E. P.; Lutz, M.; Spek, A. L.; Hage, R.; Feringa, B. L.; Munck, E.; Que, L., Jr. *Inorg. Chem.* **2003**, *42*, 2639.
(224) Balland, V.; Banse, F.; Anxolabehere-Mallert, E.; Ghiladi, M.; Mattioli, T. A.; Philouze, C.; Blondin, G.; Girerd, J.-J. *Inorg. Chem.* **2003**, *42*, 2470.
(225) At the resolution of the structure, it was not possible to say whether this was a peroxide or a superoxide intermediate.
(226) Ho, R. Y. N.; Roelfes, G.; Feringa, B. L.; Que, L., Jr. *J. Am. Chem. Soc.* **1999**, *121*, 264.
(227) Lehnert, N.; Neese, F.; Ho, R. Y.; Que, L., Jr.; Solomon, E. I. *J. Am. Chem. Soc.* **2002**, *124*, 10810.
(228) Activity is reduced 7-fold when 50 equiv of CN^- is added to wild-type SOR at 25 °C. Johnson, M. K.; Adams, M. W. W., personal communication.
(229) Romao, C. V.; Liu, M. Y.; Le Gall, J.; Gomes, C. M.; Braga, V.; Pacheco, I.; Xavier, A. V.; Teixeira, M. *Eur. J. Biochem.* **1999**, *261*, 438.
(230) Wasinger, E. C.; Davis, M. I.; Pau, M. Y. M.; Orville, A. M.; Zeleski, J. M.; Hedman, B.; Lipscomb, J. D.; Hodgson, K. O.; Solomon, E. I. *Inorg. Chem.* **2003**, *42*, 365.
(231) Lehnert, N.; Ho, R. Y. N.; Que, L., Jr.; Solomon E. I. *J. Am. Chem. Soc.* **2001**, *123*, 8271.
(232) Neese, F.; Solomon, E. I. *J. Am. Chem. Soc.* **1998**, *120*, 12829.
(233) Ho, R. Y. N.; Roelfes, G.; Hermant, T.; Hage, R.; Feringa, B. L.; Que, L., Jr. *Chem. Commun.* **1999**, 2161.
(234) Simaan, A. J.; Dopner, S.; Banse, F.; Bourcier, S.; Bouchoux, G.; Boussac, A.; Hildebrandt, P.; Girerd, J.-J. *Eur. J. Inorg. Chem.* **2000**, 1627.
(235) Simaan, A. J.; Banse, F.; Mialane, P.; Boussac, A.; Un, S.; Karger-Grisel, T.; Bouchoux, G.; Girerd, J.-J. *Eur. J. Inorg. Chem.* **1999**, 993.
(236) Simaan, A. J.; Banse, F.; Girerd, J.-J.; Wieghardt, K.; Bill, E. *Inorg. Chem.* **2001**, *40*, 6538.
(237) Horner, O.; Jeandey, C.; Oddou, J.-L.; Bonville, P.; Latour, M.-M. *Eur. J. Inorg. Chem.* **2002**, 1186.
(238) Roelfes, G.; Lubben, M.; Chen, K.; Ho, R. Y. N.; Meetsma, A.; Genseberger, S.; Hermant, R. M.; Hage, R.; Mandal, S. K.; Young, V. G.; Zang, Y.; Kooijman, H.; Spek, A. L.; Que, L., Jr.; Feringa, B. L. *Inorg. Chem.* **1999**, *38*, 1929.
(239) Burstyn, J. N.; Roe, A. R.; Miksztal, B. A.; Shaevitz, G.; Lang, G.; Valentine, J. S. *J. Am. Chem. Soc.* **1988**, *110*, 1382.
(240) Wertz, D. L.; Valentine, J. S. *Struct. Bonding* **2000**, *97*, 38.
(241) Shearer, J.; Nehring, J.; Kaminsky, W.; Kovacs, J. A. *Inorg. Chem.* **2001**, *40*, 5483.
(242) Ozaki, S.; Kirose, J.; Kidani, Y. *Inorg. Chem.* **1988**, *27*, 3746.